1969

A.C. Hall effect measurements on very high resistivity materials exhibiting electrode polarization

James Dale Boyd

Department: Physics

A.C. HALL EFFECT MEASUREMENTS ON VERY HIGH RESISTIVITY MATERIALS EXHIBITING ELECTRODE POLARIZATION

by

James Dale Boyd, 1940-

A DISSERTATION

Presented to the Faculty of the Graduate School of the

UNIVERSITY OF MISSOURI - ROLLA

In Partial Fulfillment of the Requirements for the Degree

DOCTOR OF PHILOSOPHY

in

PHYSICS

1969

Otto H. Hill
Richard Anderson
W. J. James
Eugene B. Hensley
James Paul Wesley
Norman D. Altman

ABSTRACT

A variable frequency, a.c. Hall effect measurement technique has been designed for mobility studies in very high resistivity (>10^9 ohm·cm) materials exhibiting electrode space charge polarization effects. It incorporates a neutralized input capacitance preamplifier detector which reduces the total input shunting capacitance, including the sample interelectrode capacitances, to a very low, definable value (<0.1 pf) and thereby provides very high and well defined a.c. detector input impedances (4×10^9 and 7×10^9 ohms at 600 and 200 Hz, respectively). Lumped parameter equivalent circuits have been defined to approximate the electrical behavior of sample materials in the measurement configuration. These equivalent circuits, together with independent measurements of the detector input and sample impedances, allow one to correct the detected Hall voltage and obtain the true value from which mobility data may be derived. The validity of these circuits has been established by independent a.c. and d.c. measurements on photoconductive CdS (dark resistivity >10^{10} ohm·cm) which exhibited maximum differences of less than 4%. The existing literature has been critically reviewed and the measurement criteria established by this study have been applied to resolve differences in reported data and to suggest improvements in the resolution of previously employed experimental techniques.

ACKNOWLEDGEMENTS

I wish to thank Dr. Otto H. Hill who served as my advisory committee chairman and whose many suggestions were helpful in the preparation of this dissertation. I wish to thank the state of Missouri who through the Graduate Center for Materials Research provided financial support without which this work could not have been accomplished. I wish to acknowledge the excellent assistance of Leonard A. Huneke who wrote the computer programs which greatly simplified the necessary calculations in this work. Caterpillar Tractor Co., Inc. will be warmly remembered for granting an educational leave of absence, including the fringe benefit program which afforded much peace of mind in providing medical care to my family. Finally, the Lord says in Proverbs 18:22, "Whoso findeth a wife, findeth a good thing," and I wish to acknowledge the patience of my wife, Verla, during the course of this work.

TABLE OF CONTENTS

LIST OF FIGURES

LIST OF TABLES

I. INTRODUCTION

Recent review articles by Suptitz and Teltow[1] as well as Raleigh[2] among others clearly indicate the desirability of improved experimental techniques for studying the transport properties of charge carriers in materials of interest to the fields of solid state physics and electrochemistry. Evaluation of the relative merits of theories designed to describe the interaction of charge carriers with a host lattice also requires primary data on the temperature dependence of their mobilities. In the cases of ionic conduction such data have been generated primarily by selectively doping the host material with a known concentration of appropriate impurity atoms in amounts sufficient to emphasize a particular conduction mechanism and then to determine the associated carrier mobility from conductivity measurements.

By comparison to the doping technique, Hall effect studies can provide primary data on an effective mobility when more than one charge carrier type is present, or an absolute mobility for a single carrier. However, Hall studies are difficult in ionic solids because of their typically high sample impedances over most temperature ranges of interest and the unavailability of ohmic contact electrode materials. The latter problem requires the use of a.c. techniques in order that space charge polarization

effects at the sample current electrodes may be minimized and the transverse electric field normal to the Hall electrodes be defined. Instrumentation which is adequate to minimize the effects of space charge polarization at the current electrodes and to provide adequate sensitivity for the detection of the Hall signal has been difficult to achieve, but several attempts to satisfy these requirements have been made over the past fifteen years.

Macdonald[3] developed an a.c. guarded input cathode follower detector which he and Robinson[4] used to measure the mobility of photoexcited electrons in KBr at room temperature. Onuki[5] employed a modification of the Macdonald technique to examine the mechanisms associated with the mobility of photoexcited electrons in KBr over the temperature range from 80 to 280°K. Redfield[6] developed a transient pulse, null detection technique to study photoexcited electron mobility in diamond and the alkali halides. Ahrenkiel and Brown[7] used a modification of the Redfield technique to study the low temperature mobility of photoexcited electrons in the alkali halides. Read and Katz[8] adapted a double frequency technique, first proposed by Russell and Wahlig[9] for continuous measurements on semiconductors, to measure the high temperature ionic Hall mobility of NaCl. The comparable mobility data of Onuki, and Macdonald and Robinson differ by more than a factor of two which Onuki attributes to their

oversight of the effects of detector loading. Onuki's work, on the other hand, can be shown to contain inherent compensating errors. The Redfield technique suffers from lack of sensitivity for Hall signal detection. An analysis of the Read and Katz data indicates that the frequencies employed were such that current electrode space charge polarization occurred in their measurements.

There are several requirements to be satisfied if these a.c. techniques are to be improved. First, an accurately characterized, high impedance a.c. detector exhibiting minimum shunting capacitance must be developed to monitor the Hall signal. Second, a lumped parameter equivalent circuit must be developed to represent the sample, its driving current (or voltage) source, and the Hall signal detector in order that operating frequencies may be chosen to minimize electrode space charge polarization and allow one to deduce appropriate corrections for the measured Hall signal in the presence of detector loading. Third, the validity of any proposed lumped parameter equivalent circuit must be substantiated by a set of independent measurements to assure that the mobility data deduced from this representation are truly characteristic of the sample material. The present paper describes an a.c. detection technique which satisfies the requirements outlined above. Lumped parameter equivalent circuits are proposed to define the electrical behavior of the

sample and its associated electronics. The validity of this representation is established by a series of a.c. and d.c. measurements on photoconducting CdS to which ohmic contacts can be made. On the basis of these results, the earlier referenced literature is critically examined and some of the apparent discrepancies and limitations are resolved.

II. THEORETICAL CONSIDERATIONS

Hall effect measurements represent a method of obtaining primary data on the concentration and mobility of charge carriers in electrically conducting solids. The Hall effect is based on the Lorentz force equation,

$$\vec{F} = q\vec{E} + q(\vec{v} \times \vec{B}) \qquad (1)$$

where $\vec{F}$ is the force on the particle with charge q, $\vec{E}$ is the electric field, $\vec{v}$ is the velocity of the particle, and $\vec{B}$ is the magnetic field. A typical sample for observation of the Hall effect is shown in Fig. 1.

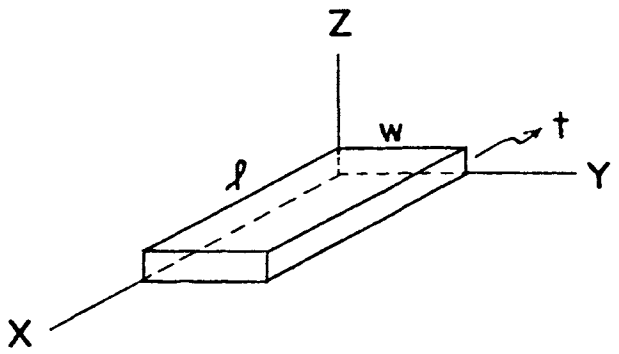

Figure 1

A typical Hall sample with dimensions of length ℓ, width w, thickness t, and coordinate axes x, y and z.

Whenever an electric field is applied in the x-direction, a velocity v_x in the x-direction is imparted to the charged particles. The Hall electric field is given by the condition $F_z=F_y=0$. The y and z components of equation (1) with $\vec{B} = B_z$ are given by:

$$F_y = qE_y + qv_xB_z = 0 \tag{2}$$

$$F_z \equiv 0. \tag{3}$$

The velocity of the charged particles is given by

$$v_x = \mu E_x \tag{4}$$

where μ is the mobility of the charge carriers. Substituting Eq. (4) into Eq. (2), we have

$$0 = E_y + \mu E_x B_z \tag{5}$$

If we now designate E_x as E_a for the applied field, E_y as E_H for the Hall field, and B as the magnetic field mutually perpendicular to E_a and E_H, Eq. (5) can be written

$$\frac{E_H}{E_a} = -B\mu = \tan\theta \tag{6}$$

where θ is defined as the Hall angle. The Hall field is the Hall voltage divided by w, and the applied field is the

applied voltage divided by ℓ.

In ionic solids to which ohmic contacts cannot be made, a space charge polarization layer is formed at the electrodes within a time scale on the order of tens of milliseconds whenever a potential is applied. This results in the generation of non-uniform electric fields within such materials upon application of d.c. potentials. Since Hall effect studies require the specification of the electric fields existing within a material, one is forced in such cases to employ a.c. techniques over a frequency range which is adequate to eliminate this polarization effect and to generate uniform electric fields throughout the material.

Hall effect studies in high impedance, ionic solids require a careful analysis of the material and the electrical detection system employed to monitor its properties. Since a.c. detectors may have relatively low input impedances compared to the impedance of a sample, it becomes necessary to apply corrections to the experimentally determined Hall voltage to account for the effects of detector loading. An equivalent a.c. circuit model for the sample must be established which allows analysis of all of the experimental conditions concerning the sample and its environment. Although it is appreciated that an exact model of a typical material sample would consist of distributed electrical parameters, such models are relatively complex and do not lend themselves to simple analysis.

One therefore attempts to define equivalent lumped parameter models which represent the distributive behavior of the sample.

An effective equivalent circuit for a high resistivity material, to which ohmic contacts cannot be made, is illustrated in Fig. 2(a). This circuit arises from the theory of Macdonald[10] for space charge limited conduction in solids. R_1 is the ordinary ohmic resistance of the sample and $X_s/2$ is the capacitive reactance of the space charge capacitance layer associated with the electrode-material interface. X_1 is the reactance of the geometric capacitance associated with the electrodes, and is affected by the sample only through its dielectric constant.

One may now consider placing the sample in series with an a.c. detector, applying a voltage V_s external to the sample, and examining the voltage V_o which will be read out by the detector. This condition is illustrated in Fig. 2(b) where R_2 and X_2 are the input resistance and capacitive reactance of the detector. The output voltage V_o is given by $V_o = F\ V_s$ where F is the transfer function defined by the combination of the sample and detector equivalent circuits. From simple circuit analysis the expression for F is

$$F = \frac{R_2(jX_2)\ (R_1 + jX_s + jX_1)}{(R_2 + jX_2)(R_1 + jX_s)jX_1 + R_2(jX_2)(R_1 + jX_s + jX_1)} \qquad (7)$$

Figure 2

Equivalent circuits used in the development of the theory. (a) a.c. equivalent circuit for a sample to which ohmic contacts cannot be made, where R_1 is the ohmic resistance, $X_S/2$ is the reactance of the space charge capacitance layer represented by C_S, and X_1 is the reactance of the geometric capacitance C_1. (b) circuit for derivation of the general transfer function where R_2 and X_2 represent the input impedance of the detector. (c) modification of (b) for detection of a Hall voltage. (d) simplified representation of circuit in (c). (e) circuit applicable when a space charge capacitance layer is present at the Hall electrodes but not at the current electrodes.

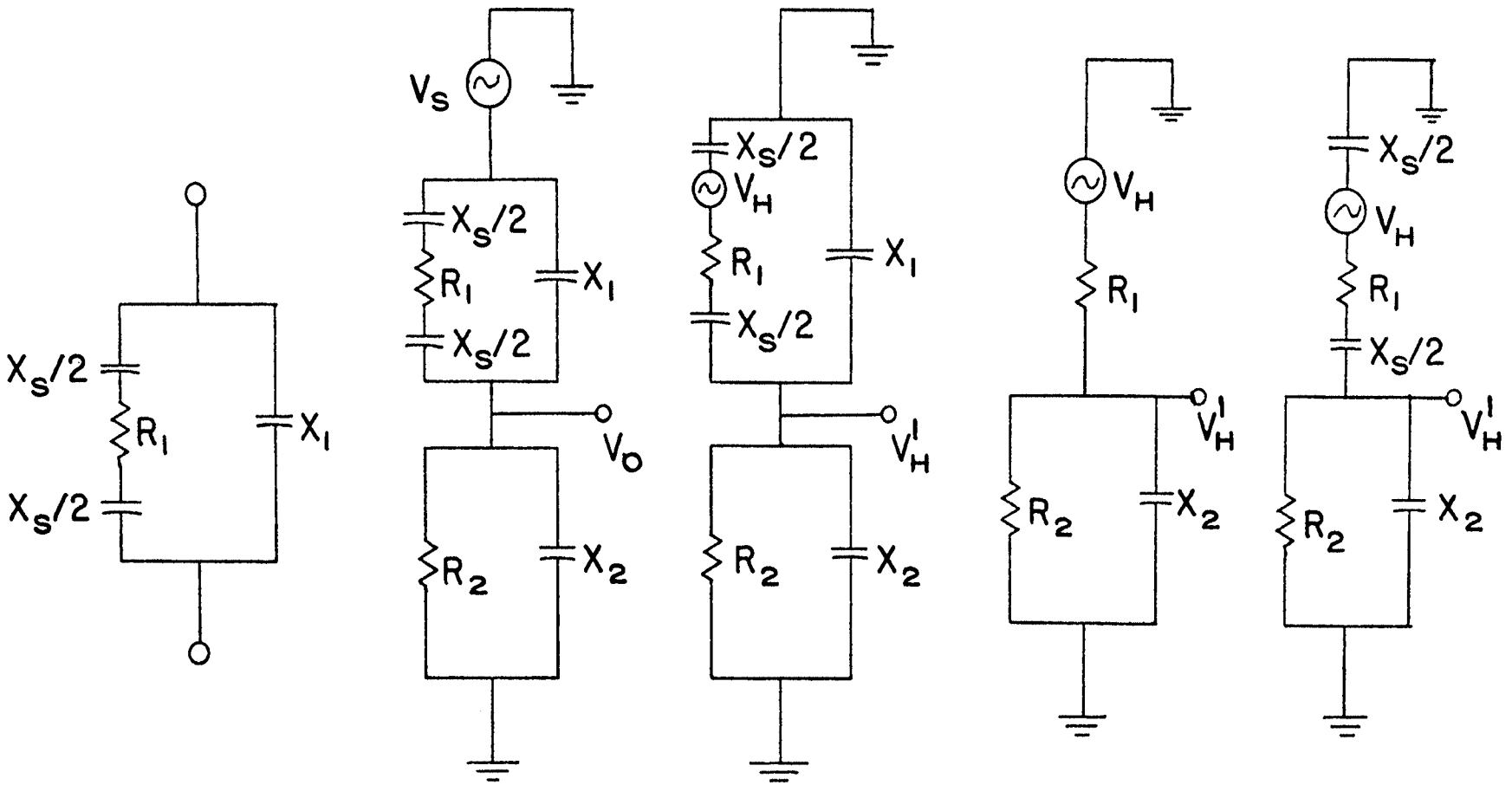
$X_S/2$
R_1
$X_S/2$
X_1
(a)
V_S
$X_S/2$
R_1
$X_S/2$
X_1
V_O
R_2
X_2
(b)
$X_S/2$
V_H
R_1
$X_S/2$
X_1
V_H'
R_2
X_2
(c)
V_H
R_1
V_H'
R_2
X_2
(d)
$X_S/2$
V_H
R_1
$X_S/2$
V_H'
R_2
X_2
(e)

Figure 2

where $X_C = -1/\omega c$, $X_L = \omega L$, ω is the radian frequency and $j = \sqrt{-1}$. Inductive reactances associated with the experimental configuration are completely negligible at the low frequencies where these measurements are usually made. Whenever $X_s << R_1$, i.e., $X_s \to 0$, F becomes

$$F_{X_s \to o} = \frac{R_2(jX_2)(R_1 + jX_1)}{R_1(jX_1)(R_2 + jX_2) + R_2(jX_2)(R_1 + jX_1)} \qquad (8)$$

The condition that $X_s << R_1$ is satisfied by using sufficiently high frequencies. This condition must be satisfied for the applied electric field to be constant along the entire length of the sample, and therefore derivable from the ratio of the voltage between the electrodes and their separation. The condition that $X_s << R_1$ can be verified by noting that the measured impedance of the sample as a function of frequency is constant over the range of frequencies used to make Hall measurements.

If one now considers the problem of detecting a Hall voltage in high resistivity materials, one must modify Fig. 2(b) to take into consideration that the equivalent Hall voltage source, V_H is internal to the sample. The resultant equivalent circuit is illustrated in Fig. 2(c). The equivalent Hall voltage generator impedance has no capacitive component, and therefore, the Hall voltage source appears only in the resistive portion of the

equivalent circuit representing the sample. This is true because a Hall voltage is established by the charge gradient produced by the motion of the charge carriers in the crossed E and B fields. This motion is dependent upon the transport properties of the charge carriers and not a priori on the dielectric constant. In other words, if one had two materials with identical transport properties but different dielectric constants, the generated Hall voltage would be the same value in each material. The detected Hall voltage V_H' would not necessarily be the same due to the difference in the shunting effect of C_1, whose value would be different for the two materials because of their different dielectric constants.

Notice that X_1 now appears as a shunt from the input of the detector to ground and can therefore be included in X_2. At this point it should be emphasized that X_2 contains all the reactive impedance which shunts the detector to ground. With this in mind, and with $X_s << R_1$, the circuit of Fig. 2(c) becomes that illustrated in Fig. 2(d). This is the circuit that will be used in making the corrections necessary for detector loading in this work. Comparing this circuit to that in Fig. 2(b), one sees that the transfer function for this circuit is obtained by letting $X_s \rightarrow 0$ and $X_1 \rightarrow \infty$ in the general transfer function F derived for the circuit of Fig. 2(b). The expression for

$F_{X_s \to 0,\ X_1 \to \infty}$ after being rationalized is given by

$$F_{X_s \to 0,\ X_1 \to \infty} = \frac{(X_2R_2)^2 + X_2^2 R_1R_2 + j(R_2^2R_1X_2)}{(X_2R_2 + X_2R_1)^2 + (R_1R_2)^2} \qquad (9)$$

Under certain conditions, in some materials it might be possible that a space charge condition could exist at the Hall electrodes and not at the current electrodes since the Hall electrodes are usually smaller in area and may exhibit correspondingly smaller capacitance than that at the current electrodes. Therefore, $X_s << R_1$ is not as easily satisfied at the Hall electrodes as it is at the current electrodes. If this condition did exist, it would be possible to determine C_s and thus $X_s = -1/\omega C_s$ by analyzing the frequency dependence of the real part of an independent admittance measurement of the sample at the electrodes of interest. The admittance of the sample equivalent circuit in Fig. 2(a) is given by

$$Y = \frac{S_s^2 G_1}{G_1^2 + S_s^2} + \frac{jS_s G_1^2}{G_1^2 + S_s^2} + jS_1 \qquad (10)$$

where $S_s = \omega C_s$, $S_1 = \omega C_1$ and $G_1 = 1/R_1$. The real part of Y is frequency dependent and measurements at two frequencies would serve to define C_s and R_1. Figure 2(e) illus-

trates the equivalent circuit which would apply to the detection of a Hall voltage if the Hall, but not the current, electrodes exhibit a space charge capacitance layer at the frequency of measurement. Again comparing this circuit to that of Fig. 2 (b), one observes that its transfer function is given by

$$F_{X_1 \to \infty} = \frac{jR_2X_2}{(R_2 + jX_2)(R_1 + jX_s) + jR_2X_2} \tag{11}$$

The frequency dependence of eqn. (11) is more readily analyzed in the following form

$$F_{X_1 \to \infty} = \frac{j\omega R_2 C_s}{R_1R_2C_sC_2\left[\frac{1}{R_1R_2C_sC_2} + j\omega\frac{(R_2C_2 + R_1C_s + R_2C_s)}{R_1R_2C_sC_2} - \omega^2\right]} \tag{12}$$

upon substitution of the relations $X_2 = -1/\omega C_2$ and $X_s = -1/\omega C_s$.

Since the true Hall voltage V_H can be found from $V_H' = V_H F_{X_S \to 0, X_1 \to \infty}$, the problem is now reduced to one of determining the parameters which make up the transfer function. Figure 3 is a schematic representation of a typical Hall sample where terminals 3 and 5 are the current electrodes and 1 and 4 are the Hall electrodes. There is a geometric capacitance between each electrode and ground

Figure 3

Typical Hall sample configuration showing the current electrodes (3 and 5) and the Hall electrodes (1 and 4). The driving generator is represented by two voltage sources $V_a/2$, 180° out of phase, each with an internal impedance of R_s.

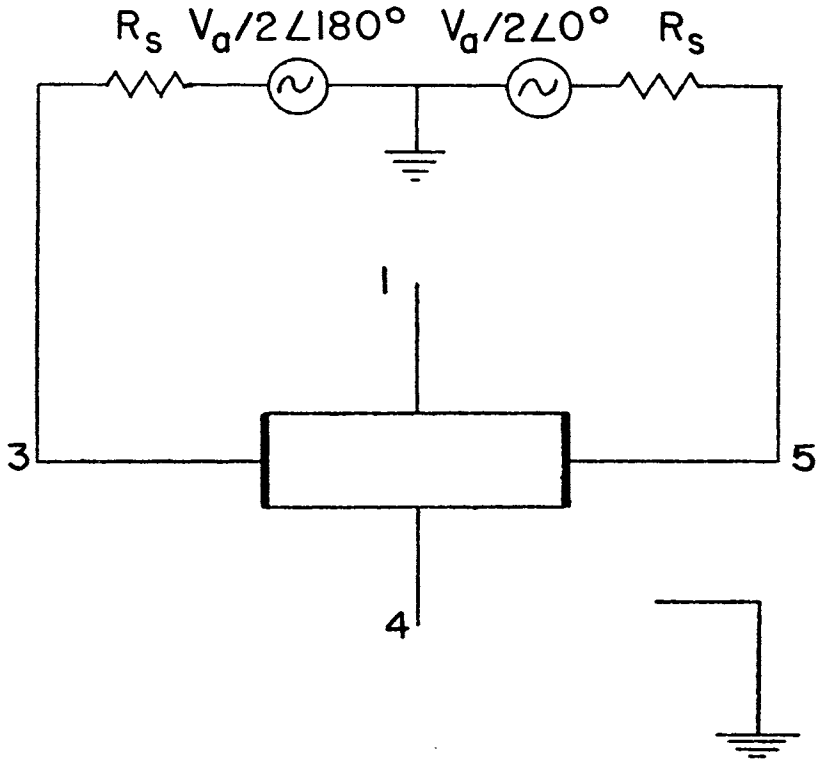

Figure 3

and a mutual geometric capacitance between the electrodes themselves, each of which will be indicated by the appropriate subscripts. Experimentally, it is easier to implement the measurement and the parameters are easier to analyze if electrodes 3 and 5 are driven 180° out of phase and a single ended detection system is used with electrode 4 grounded and electrode 1 as the input detector. By grounding terminal 4, capacitance C_{4g} is immediately of no consequence and C_{14} becomes part of C_{1g}. Capacitances C_{3g}, C_{5g}, and C_{35} cause no difficulties as long as X_{3g}, X_{5g}, and X_{35} are large compared to the source impedance R_s of the driving voltage generator V_a which is connected to the terminals 3 and 5. This condition is always and easily satisfied. Capacitance C_{1g} returns directly to ground, while C_{13} and C_{15} return to ground through the driving generator impedance, R_s, which is small compared to X_{13} and X_{15}. These capacitances, therefore, constitute a capacitive shunt to ground across the detector and become part of the detector input impedance which enters the expression for $F_{X_S \to 0,\ X_1 \to \infty}$ as X_2. The Hall source generator resistance R_1 and the geometric capacitances C_{1g}, C_{13}, and C_{15} must be determined by independent measurements. The detector input impedance must also be determined by separate measurements. The quantities in the transfer function are these: R_1 the Hall source resistance, R_2 the detector input resistance, and X_2 the detector

shunt reactance made up of the detector input capacitance C_d and the geometric capacitances C_{1g}, C_{13}, and C_{15}. Thus, all quantities in $F_{X_S \to 0,\ X_1 \to \infty}$ are independently determined as they must be to make properly any corrections necessary for the effects of detector loading.

Capacitance C_{13} and C_{15} also form a path from the driven current electrodes to the high impedance detector ($\simeq 5 \times 10^9$ ohms) causing a "misalignment" voltage to appear which is indistinguishable from a Hall signal. If C_{13} and C_{15} were ideally equal, no such voltage would appear. In general, since this is impossible to achieve, it is best to make C_{13} and C_{15} as small as possible in order to minimize this signal and thus reduce the problem of eliminating this "misalignment" voltage. These capacitances are considerably reduced by placing the sample holder within an external grounded shield and thus creating a three-terminal capacitor whose value is proportional to $e^{-Az/r}$ where A is a constant, z is the plate separation, and r is the radius of the shield.[11] For any given plate separation z of the order of the plate size or greater, a three terminal capacitor has much less capacity than the unshielded type in which the capacitance is proportional to 1/z.

It is normal procedure when discussing the Hall effect to refer to the Hall coefficient defined by $R = E_H/JB$,

where J is the current density flowing in the sample. Implicit in the definition of R is the assumption that the current in the sample is supplied by a current source which ideally has an infinite source impedance in relation to the sample impedance. In practice, this is not always attainable, and with high resistivity materials the driving source most often appears as a voltage source to the sample and not a current source. A more fundamental specification of the mobility which avoids the error of implicitly assuming a current driving source is obtained from the measurements of the Hall angle θ given by Eq. (6). If single ended detection is used and the driving source appears as a voltage source rather than a current source to the sample, then only one half of the Hall voltage will be detected as the following explanation will show.

Figure 4 (a) illustrates a Hall sample in a measurement configuration with the lumped equivalent Hall generators and their source resistances superimposed upon it. It is necessary to split the equivalent Hall generator into two identical sections because of the symmetry of the sample in the longitudinal direction, i.e., the direction of the applied electric field. Voltages V_1 and V_2 are each one half of the Hall voltage V_H, each having a source resistance R_H. Figure 4 (b) shows only the lumped equivalent portion of the configuration in Fig. 4 (a), without the sources $V_a/2$ but with their source resistances R_S included, in

Figure 4

(a) A Hall sample in a Hall measurement configuration with the lumped equivalent Hall source generator and its source resistances R_H superimposed upon it. $V_1 = V_2 = V_H/2$. Z_D = detector input impedance. (b) Lumped portion of (a) redrawn in a simplified manner without V_S to show the effects of R_S on the voltage V_H detected across Z_D.

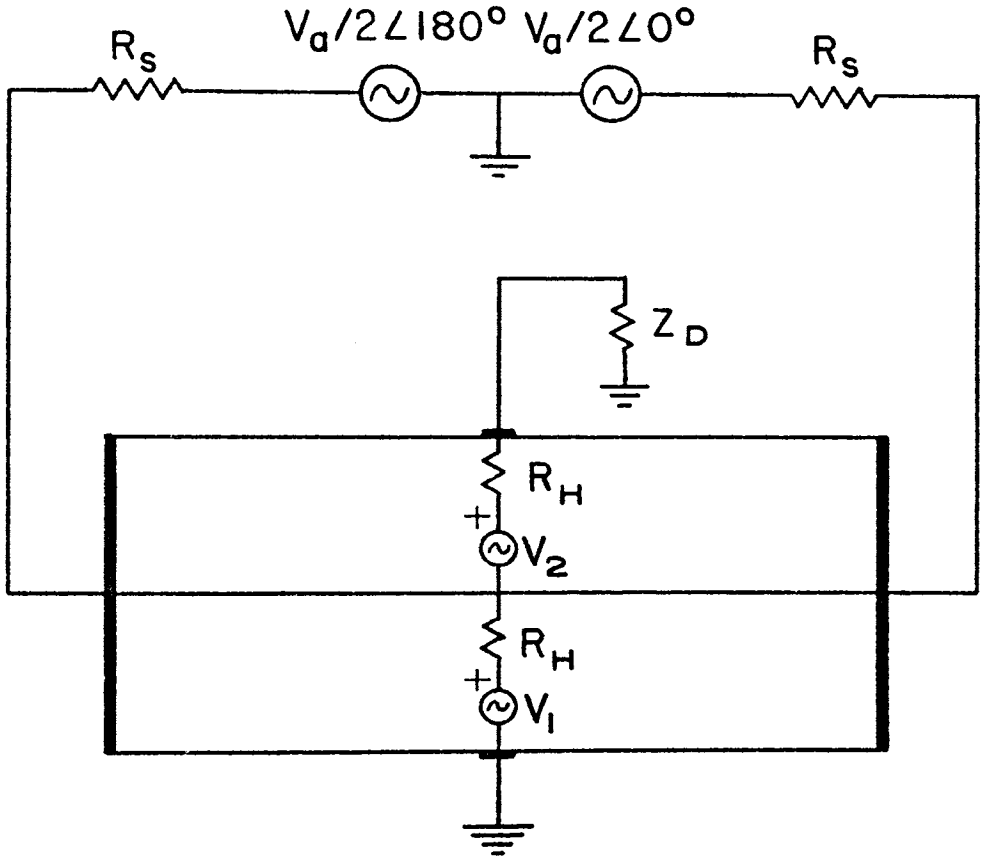

(a)

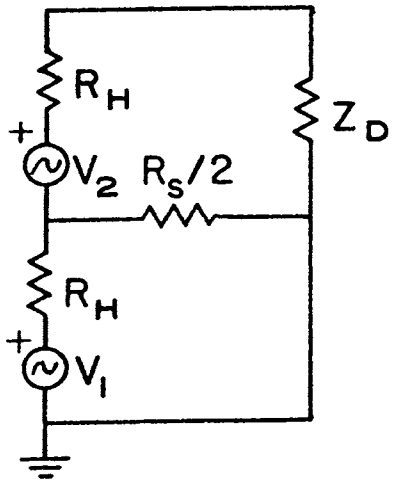

(b)

Figure 4

order to examine the effects of the various impedances in the circuit upon the detected Hall voltage V_H'.

One must now determine what voltage V_H', due to V_1 and V_2, appears across Z_D, the detector input impedance, for it is at this point that the Hall voltage is detected. Using the principle of superposition and solving for V_H', one finds

$$V_H' = \frac{V_1 Z_D R_S/2 + V_2(R_H + R_S/2) Z_D}{(R_H + R_S/2)(R_H + Z_D) + R_H R_S/2} \tag{13}$$

However, when $R_S << R_H$, i.e., when the driving source looks like a voltage source to the sample, there is no contribution to V_H' from V_1 and the expression above reduces to

$$V_H' = V_1 \cdot (0) + \frac{V_2 Z_D}{R_H + Z_D} \tag{14}$$

Thus, since $V_1 = V_2 = V_H/2$, only one half of the Hall voltage will be detected, still subject, however, to possible correction due to detector loading. This result has been verified experimentally with both the a.c. and d.c. methods for making Hall measurements. Whenever a single ended detection system is used for high resistivity materials, the second Hall electrode (#4 in Fig. 4 (a)) should not be used in order to insure that only 1/2 of the Hall voltage is detected regardless of the relative values of R_S and R_H. The Hall generator resistance R_H now must be

determined by an impedance measurement on the sample between terminal 1 and terminals 3 and 5 which are tied together. This resistance is the resistance R_1 in the transfer function used to correct for detector loading effects. Whenever the driving source appears as a current source to the sample ($R_S >> R_H$), the full Hall voltage will be detected with electrode 4 grounded.

The preceding discussion also indicates that the analysis of a balanced detection system is reduced to the analysis of two single ended detection systems, each of which detects one half of the Hall voltage in the limit of no detector loading.

Whenever one encounters very high impedance, such as those in ionic solids, even in the photo-conducting state, consideration should also be given to sample size in order to optimize the experiment. Since one desires C_{13} and C_{15} to be as small as possible, typical sample cross sectional areas of 0.1 to 0.5 cm^2 indicate that sample lengths should be of the order of 1 cm in the three terminal configuration. The typical cross sectional areas quoted are somewhat larger than those of typical Hall bars. However, they are especially advantageous whenever ohmic contacts cannot be made to a specimen, precluding a four-point conductivity measurement. This requires that conductivity data be obtained from the impedance measurement across the current electrodes of the sample. Increased

width and thickness reduce the sample impedance and make better impedance measurements possible, thus improving the data for conductivity. Good results have been obtained with bridge measurements. Increased width also increases the size of the Hall voltage to some extent, which in some instances can be an advantage.[12]

In summary, these theoretical considerations require that:

a) independent measurements be made of the equivalent Hall voltage source resistance.

b) independent measurements be made to determine capacitive effects of the electrode structure of the Hall sample.

c) impedance measurements vs. frequency be taken to establish that $X_s << R_l$ at the current and Hall electrodes. If this is not true at the Hall electrodes, then C_s and R_l must be determined for use in the appropriate transfer function. If it is not true at the current electrodes, then accurate measurements are precluded.

d) it be established whether the driving source appears as a voltage or a current source to the sample since this influences both the portion of the Hall voltage detected and capacitive loading effects of the electrode structure.

e) the detector input impedance be established at each frequency of interest in terms of a parallel R,C equivalent circuit.

III. EXPERIMENTAL APPARATUS AND PROCEDURE

The first problem to be resolved for making a.c. Hall effect measurements on very high resisitivity samples was the design of a detection system with sufficiently high input impedance, which is difficult to achieve because of the customarily high detector shunting input capacitance. Attempts to reduce the detector input capacitance have been made by Macdonald,[3] who developed a guarded input, unity gain , a.c. cathode follower circuit which exhibited an effective input resistance of 4×10^9 ohms shunted by a 0.3 picofarad input capacitance over the frequency range extending up to 4KHz. Any additional sample geometric capacitance must be added to the detector capacitance in this mode of operation. Onuki,[5] using similar circuitry quoted an input impedance for his detector of 80MΩ at 330Hz and suggested that a detector loading correction of the form $Z_{in}/(Z_{in} + Z_{cry})$ must be made in both his work and that of Macdonald. Neither of these detection techniques were applied to sample systems in which the a.c. results could be compared directly with data obtained in the d.c. mode.

In surveying available commercial detection equipment, it was learned that preamplifiers utilizing positive, variable capacitive feedback have been used in bio-medical research for some time to make measurements of single-cell activation potentials through high impedance electrodes.

This positive feedback appears as negative capacitance at the input, which, when added to the capacitance shunting the input, reduces it to a very low value. After examining the specifications of several units made by different manufacturers, three units were secured on loan for evaluation; two consisted of models ELSA-1 and ELSA-3 manufactured by Electronics for Life Sciences of Rockville, Maryland, and one was Model NF-1, manufactured by Bioelectric Instruments, Inc., of Yonkers, New York.

A comparative study was made of the ability of these instruments to detect signals from high impedance sources. Since positive feedback is employed, these amplifiers become unstable and oscillate when the feedback is increased beyond a critical limit. The minimization and reproducibility of the input shunting capacitance depends sensitively upon the sharpness of the critical tuning limit which was monitored by an oscilloscope. Furthermore, if the frequency of the induced oscillation occurs in the frequency range being employed in sample measurements, the onset of oscillation appears as a continuous increase in the amplitude of the monitored signal making precise definition of optimum tuning practically impossible.

Of the units examined, the Bioelectric Model NF-1 exhibited the most sharply defined tuning properties. The frequency of oscillation of each of the units depended upon the source impedance and decreased with increasing source

impedance. The ELSA units were found to oscillate with a frequency which fell in the 200-600 Hz contemplated for these studies, while the Bioelectric NF-1 oscillated at frequencies above 1.5KHz for all values of source impedance employed. On the basis of this examination, the Bioelectric NF-1 was chosen for incorporation into the measurement system.

Capacitances in the amount of $C=(1-G)C_f$ can be neutralized with the NF-1, where G and C_f are the amplifier gain and feedback capacitance, respectively. C_f is variable up to 25 picofarads, and the manufacturer recommends that for this mode of operation the gain not be set above 5. All measurements were made at a gain of 3. Therefore, the instrument was capable of neutralizing most of the capacitance of a reasonable length cable and presented a very high impedance at the sample electrodes. A ten-turn drive was added to the simple parallel-plate neutralization capacitor, C_f, in order to improve the tuning resolution.

A second important problem concerns the description of the circuit parameters with sufficient precision to allow one to deduce the electrical properties of interest. It should be noted that in the present mode of operation the NF-1 neutralized all input shunting capacitance between the sample electrodes and the detector to the limiting minimum value obtainable prior to the onset of oscillation(0.085 pf). Thus, a simple measurement of the input resistance R_2 and

the input capacitance C_2 shown in Fig. 2(d) was sufficient to specify the transfer function at a particular frequency. Independent measurements of the other components of C_2 [C_{1g}, C_{13} and C_{15} (Fig. 3)], are not required since these contributions are all subject to neutralization by the NF-1. Other modes of detection, such as a guarded input preamplifier, neutralize only the detector input capacitance, C_d, and the unneutralized contributions from C_{1g}, C_{13} and C_{15} are not only large (>1pf), but must be precisely and independently measured to evaluate C_2 for use in the transfer function of interest.

A very high impedance, precisely characterized source was required to evaluate the assumed R_2, C_2 parallel equivalent input impedance of the amplifier. This was provided by an especially constructed adjustable three-terminal capacitor used in series with the variable phase function generator which served as the a.c. signal source in all of the present work. The arrangement was exactly as shown in Fig. 2(b) with the conditions that $R_1 \to \infty$, $X_s \to o$ and $C_1 = 0.00980$pf, which was the value of the source capacitance as monitored with the GR 1615-A impedance bridge. The specified accuracy of the GR 1615-A for this type of measurement is $\pm$ (0.01% + .00003 pf) which, when applied to the value for C_1, yielded $C_1 = 0.00980 \pm 0.00013$ pf. Whenever the coupling of the amplifier through a capacitive source was sufficiently great, the behavior of the amplifier was

not precisely defined. It was found that for best results, C_1 should be at least 1/5 the value of the least equivalent input capacitance that can be obtained at the amplifier input ($\simeq$ .05 pf).

To evaluate the frequency dependent parameters R_2 and C_2, one measures the ratio of output to source voltage, V_o/V_s [Fig. 2(b)] at frequencies displaced 25Hz on each side of the frequency of interest. The values of R_2 and C_2 are then found from the solution of the two simultaneous equations

$$\left| \frac{V_o}{V_s} \right|_{\omega_1} = \left| F_{R_1 \to \infty,\ X_s \to o} \right|_{\omega_1} \tag{15}$$

$$\left| \frac{V_o}{V_s} \right|_{\omega_2} = \left| F_{R_1 \to \infty,\ X_s \to o} \right|_{\omega_2} \tag{16}$$

where $F_{R_1 \to \infty, X_s \to o}$ is the general transfer function of Eq. (7) simplified for the conditions $R_1 \to \infty$, $X_s \to o$, and $C_1 = 0.00980 + 0.00013$ pf as measured on the GR 1615-A capacitance bridge. A computer program was written to solve these equations since they were somewhat complicated.

The frequency range from 200 to 600Hz was chosen for these measurements because the elimination of electrode

blocking, $X_s << R_l$, was satisfied in this range, and the detector input impedance was acceptable. Macdonald and Robinson[4] indicate that any frequency above 30Hz satisfied this condition for Hall measurements on KBr. Onuki[5] estimates that C_s is 150 pf/cm^2 for KBr and with the typical cross sectional areas and sample resistances that he employed, the condition is satisfied for frequencies of the order of 100Hz. The data of Kahn and Glass[13] on the photocapacitive effect in KBr show that a frequency of 50Hz would be completely sufficient.

A block diagram of the Hall measurement system is shown in Fig. 5. A Model 203A Hewlett Packard Variable Phase Function Generator is employed as the voltage source. It provides two sinewave outputs, with individual amplitude controls. Output B drove electrode #3 on the sample, and its phase, which is continuously adjustable with respect to that of output A, was normally run at 180° with respect to output A, which drove electrode #5 on the sample. The charge carrier type was determined by the phase of the Hall signal from electrode #1 (Fig. 5) relative to the applied signal at electrode #5 (Fig. 5). The phase relationship was indicated by the lock-in-amplifier which derived its reference signal from output A, i.e., current electrode #5 (Fig. 5). Notice in Fig. 5 that electrode #4 was not used since single ended detection was employed and the driving source appeared as a voltage source to the sample. In

Figure 5

Block diagram of the Hall effect measurement system. a) Variable phase, variable frequency oscillator. b) Sample. c) Neutralized input capacitance preamp. d) Lock-in amplifier. e) Strip-chart recorder. f) Wave analyser. g) Oscilloscope. h) Environmental chamber.

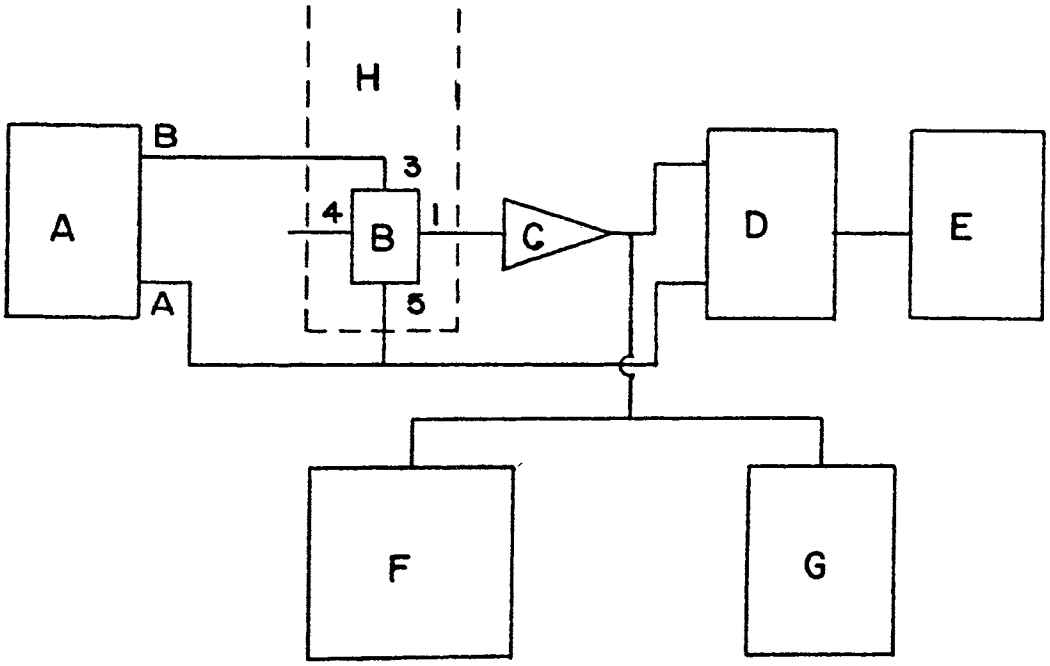

Figure 5

general, it is impossible to make C_{13} and C_{15} equal and to exactly align the Hall electrodes, particularly with high impedance samples, and a "misalignment" voltage appears at the preamplifier (NF-1) which must be eliminated. This false signal was removed by making minor adjustments in the amplitude and phase, about 180°, of output B of the driving generator. A ten-turn drive was added to the phase control on the function generator to achieve the phase resolution required by these very small adjustments. A fine amplitude control was added in the line from output B and consisted of a ten-turn 10KΩ potentiometer in series with a 50KΩ fixed resistor which gave resolution equivalent to a sixty-turn potentiometer.

The quality of the null of the "misalignment" voltage depended substantially upon the sample impedance level and improved as the sample impedance decreased. The overall stability and quality of the entire system was determined by setting up the conditions as they were just before the magnetic field was applied and obtaining a recorder tracing at the output of the lock-in-amplifier which showed the stability and noise level of the system. The zero magnetic field, i.e., zero Hall signal baseline, was determined from this tracing and the uncertainty in establishing the baseline was taken as the minimum Hall signal $V_H(min)$ which would be required for a signal-to-noise ratio of one. Figure 6 presents typical tracings showing stability and

Figure 6

Recorder tracings of the output of the lock-in amplifier showing the noise level and stability of the system. a) V_a = 7.66 volts, R = 10^5 Ω, T = 3 sec. b) Va = 7.66 volts, R = 10^6Ω, T = 1 sec. c) V_a = 7.27 volts, R = 10^7Ω, T = 300 ms. d) V_a = 7.61 volts, R = 10^8Ω, T = 1 sec. e) V_a = 7.61 volts, R = 10^9Ω, T = 1 sec. T is the filter time constant on the lock-in amplifier. V is the applied voltage between the current electrodes. R is the equivalent source impedance which the preamplifier sees. All time scales are identical as marked.

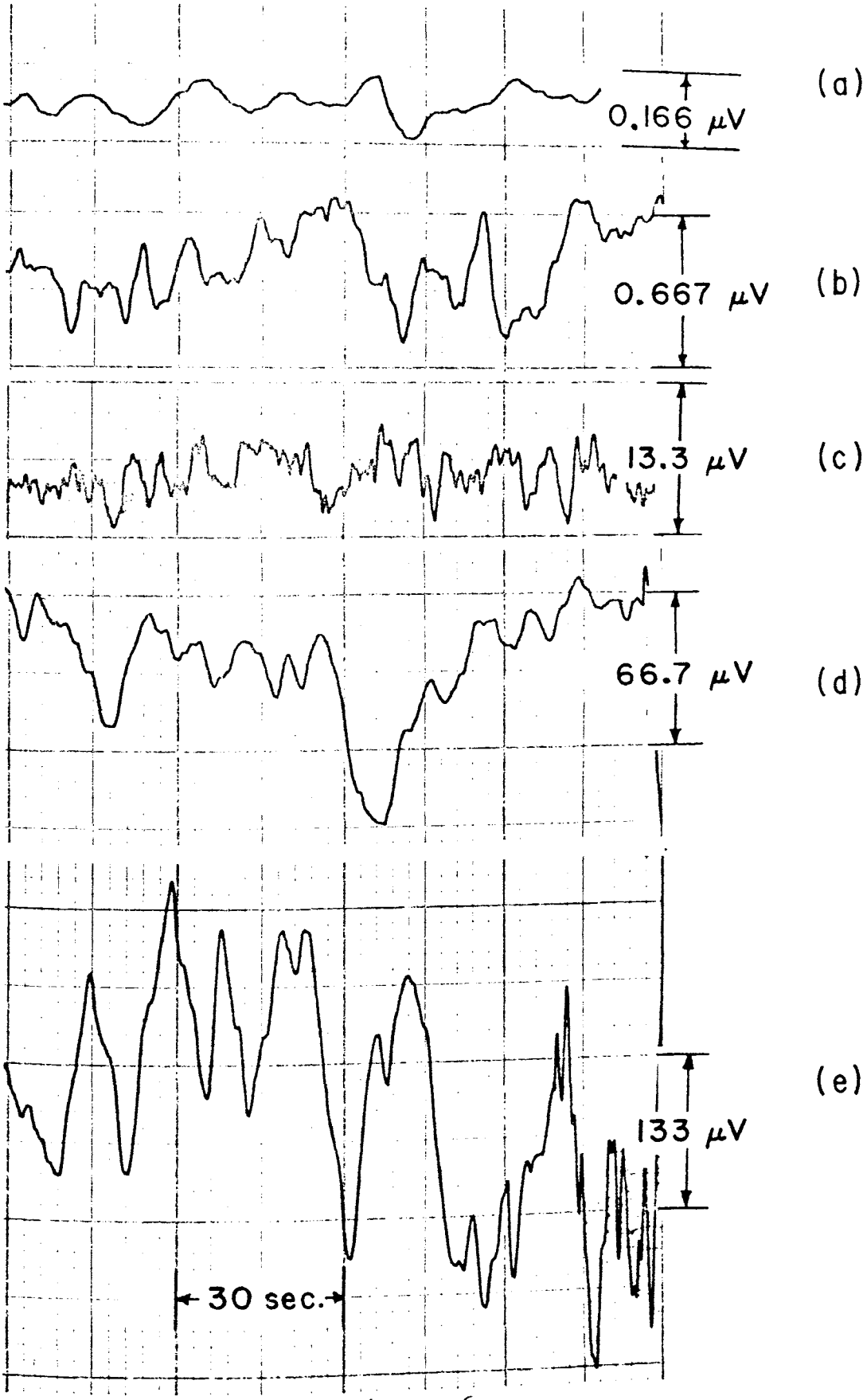

Figure 6

noise level at various impedance levels for the system under the conditions described above. Tabulated in Table I are the values of $V_H(min)/V_a$, which is a good quantity to use to specify the system capability. One, of course, must realize that individual sample properties can alter significantly the uncertainty in determining the baseline. This would be especially true if the sample was to demonstrate short term instabilities which would force one to use a shorter time constant at the lock-in-amplifier, thus widening the noise bandwidth. These short term sample variations can arise from slight inhomogeneous changes in the sample and can be attributed to small temperature fluctuations, surface contamination effects, small changes in electrode properties, mechanical vibration, etc.

The principle source of the noise in the system as shown in Fig. 6 was due to amplitude and/or phase "jitter" between outputs A and B of the function generator. Figure 7 shows a tracing of the output of a differential amplifier (Keithley Model 603) which monitored the difference (A-B) between the outputs A and B of the driving generator. The total deviation of Fig. 7 represents approximately 5 parts in 10^5 of the voltage between the outputs A and B. If one uses the same technique employed to establish a baseline for the system, the generator differential amplifier combination alone produces an equivalent, "$(V_H(min)/V_a)$" = 4×10^{-6}, which is about the same as the high impedance

TABLE I

Tabulation of the minimum Hall Signal, $V_H(min)$, required for a signal-to-noise ratio of one. The ratio $V_H(min)/V_a$ is given to show the effects of various impedance levels. The applied voltage V_a and the impedance level R given are the ones used in obtaining the tracings of Fig. 6 from which $V_H(min)$ was determined.

R(ohms)	$V_H(min)\mu V$	V_a (volts)	$V_H(min)/V_a$
10^5	0.02	7.66	2×10^{-9}
10^6	0.07	7.66	9×10^{-9}
10^7	1.3	7.27	1.8×10^{-7}
10^8	6.7	7.61	8.7×10^{-7}
10^9	13	7.61	1.7×10^{-6}

Figure 7

Recorder tracing of output of lock-in amplifier with input signal from a differential amplifier which monitored the difference (A-B) between the two outputs of the function generator which served as the driving source. Applied voltage V_a between differential amplifier inputs is 1.00 volts. Lock-in amplifier time constant T = 300 ms. Compare with Fig. 6(c), which also has T = 300 ms, to notice that the character of the noise in the system is identical to that in the function generator.

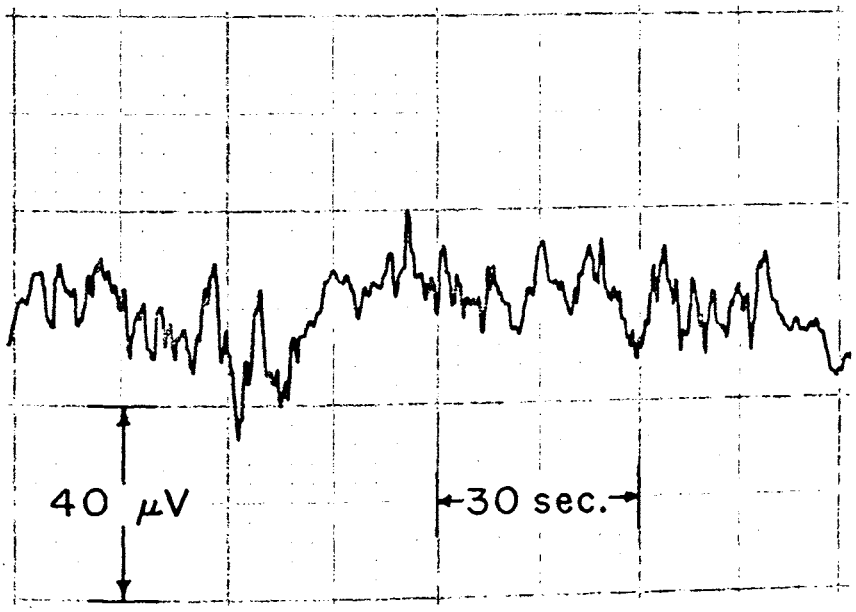

Figure 7

value in Table I. Thus, one can see that this was the major source of "noise" in the system.

Because of the neutralization feature of the preamplifier, rigid mounts had to be built such that there was no relative movement between the sample chamber and the preamplifier. Any relative movement caused the short interconnecting cable to flex, and thus, to produce a small but definite change in the cable capacitance. This changed the tuning of the preamp, and therefore, produced a change in the output voltage. This voltage was indistinguishable from a Hall voltage with respect to the rest of the analyzing equipment and had to be eliminated. The mounts for the preamplifier and the sample chamber were constructed from 5/8" aluminum plate. These were bolted to a 1½" aluminum plate which formed part of the base for the magnet, and relative movement between the preamp and the chamber was limited to less than .001" under all conditions, which was sufficient to eliminate this source of error in the Hall signal. Figure 8 shows the final form of the experimental assembly.

The sample holder was constructed out of commercial teflon with movable tabs which contained the electrodes. These tabs were spring loaded to insure contact with the sample. The Hall leads were shielded to within 2 mm of the Hall electrodes, and the current leads were shielded to within 6 mm to reduce the interelectrode capacitances to

Figure 8

Final experimental assembly showing required construction to eliminate relative movement between the sample chamber and the preamplifier. Marked in the photograph is the Bioelectric Model NF-1 preamplifier (a), and the ten-turn drive (b) which was added to the preamp feedback capacitor C_f for improved tuning resolution, and the end of the sample chamber (c) which extends between the magnet pole faces. Also marked is the small vacuum system consisting of the roughing value (d), the up-to-air value (e), and the 11 liter per second ion pump (f).

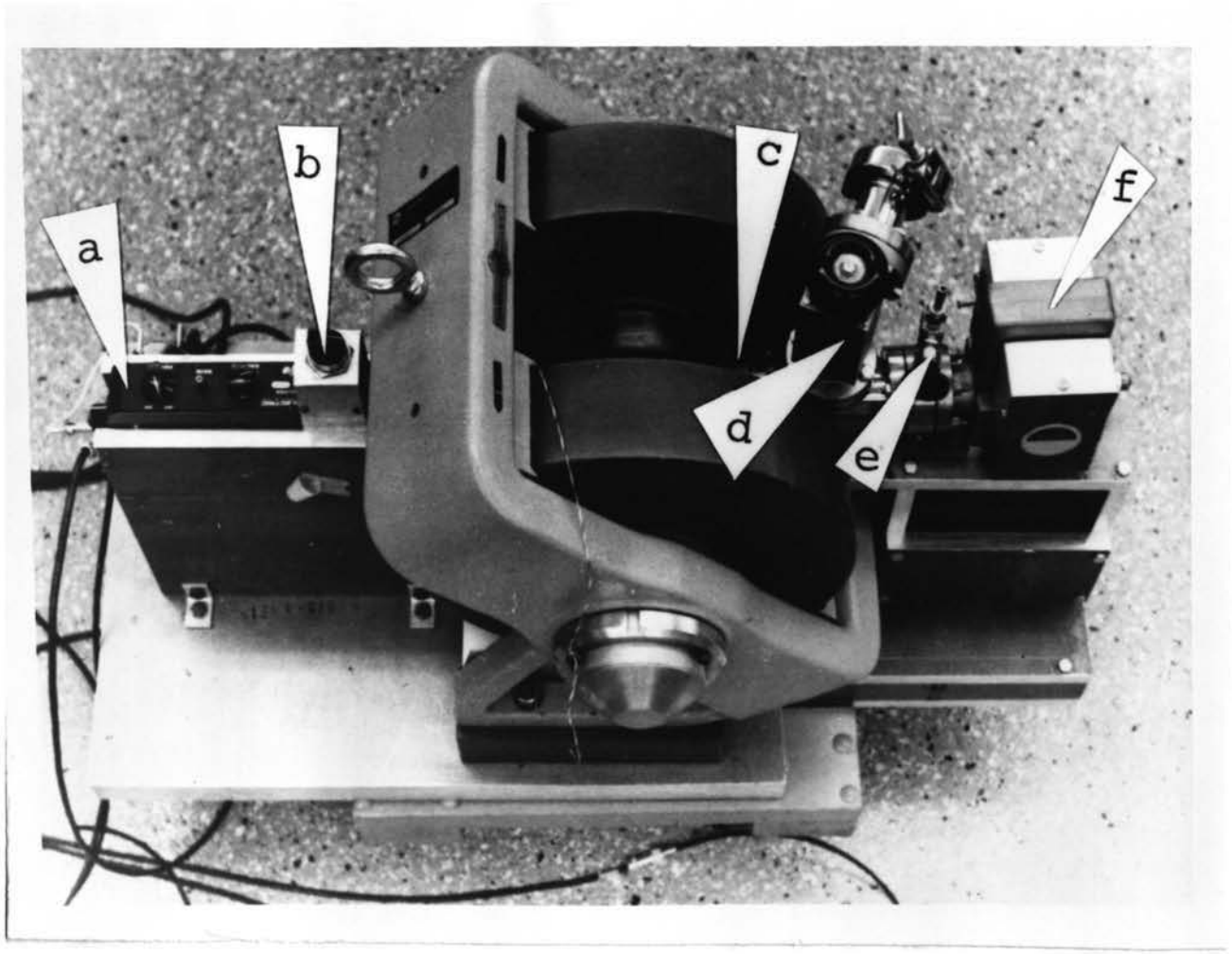

Figure 8

a minimum. A photograph of the sample holder assembly is presented in Fig. 9. The leads are spotwelded to the electrodes and come through a nine pin feed through on a vacuum flange to which the entire sample holder was mounted. This unit was placed into a 1" square , non-magnetic, stainless steel tube, which had a mating flange connected to a small 11 liter per second ion pumped vacuum system and served as an absolute electrical shield and environmental chamber. All materials are non-magnetic. The overall system electrical shielding was sufficient to eliminate all detectable 60Hz pickup. The entire sample chamber and its integral vacuum chamber were sufficiently small to be accommodated in commercial, controlled environmental glove boxes for sample loading purposes. The experimental assembly was constructed to accommodate a wide variety of sample materials. For the present work, environmental integrity was not a strict requirement and the vacuum system was not employed. Only the 1" square sample chamber was used to provide the necessary shielding against 60Hz pickup. The magnetic field required for the Hall measurements was provided by a 4 inch diameter pole face Varian model V-4000 variable gap electromagnet. Fields exceeding 10 Kilogauss could be obtained with a one inch gap. Magnetic field calibration was provided to within one percent by a Bell Gaussmeter Model 120.

a minimum. A photograph of the sample holder assembly is presented in Fig. 9. The leads are spotwelded to the electrodes and come through a nine pin feed through on a vacuum flange to which the entire sample holder was mounted. This unit was placed into a 1" square , non-magnetic, stainless steel tube, which had a mating flange connected to a small 11 liter per second ion pumped vacuum system and served as an absolute electrical shield and environmental chamber. All materials are non-magnetic. The overall system electrical shielding was sufficient to eliminate all detectable 60Hz pickup. The entire sample chamber and its integral vacuum chamber were sufficiently small to be accommodated in commercial, controlled environmental glove boxes for sample loading purposes. The experimental assembly was constructed to accommodate a wide variety of sample materials. For the present work, environmental integrity was not a strict requirement and the vacuum system was not employed. Only the 1" square sample chamber was used to provide the necessary shielding against 60Hz pickup. The magnetic field required for the Hall measurements was provided by a 4 inch diameter pole face Varian model V-4000 variable gap electromagnet. Fields exceeding 10 Kilogauss could be obtained with a one inch gap. Magnetic field calibration was provided to within one percent by a Bell Gaussmeter Model 120.

Figure 9

Close up view of sample holder showing the shielding of the leads, the adjustable spring loaded teflon tabs, the current electrodes 3 and 5, and the Hall electrodes 1 and 4.

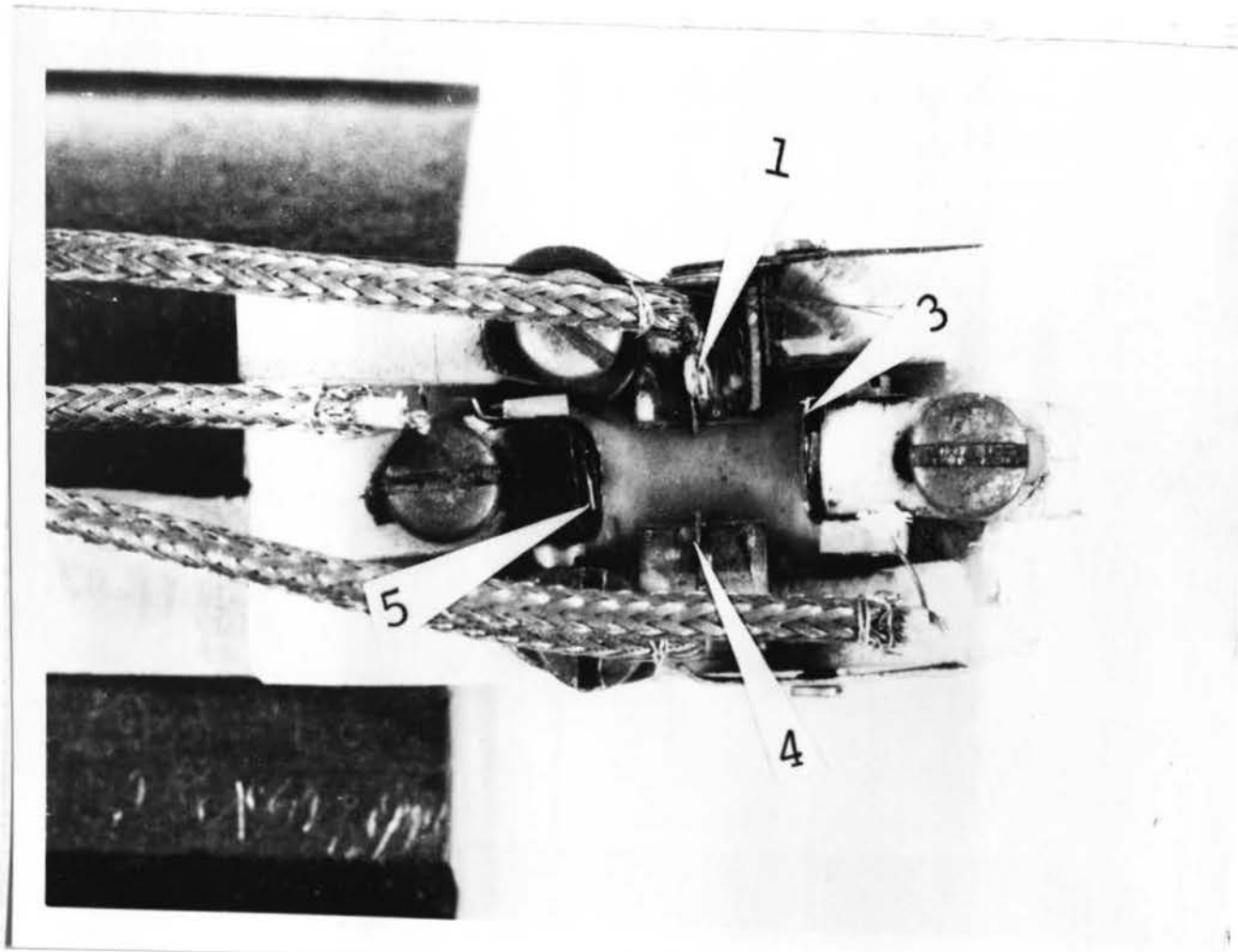

Figure 9

Once the electronic signal detection circuitry was designed and characterized and the experimental assembly was constructed and checked out, it was then possible to address oneself to the question of establishing the validity of the lumped parameter equivalent circuit description employed for analyzing the Hall effect properties of sample materials. A comparison of a.c. and d.c. generated Hall voltage data on a single material was considered to be the most significant test of the models and analytical methods proposed for the a.c. method. A sample material of high and preferably variable resistivity to which ohmic contacts could be made was required for this comparison.

An unoriented crystal of cadmium sulfide (CdS) having dimensions of 9.99 x 4.34 x 104 mm was obtained from Clevite Corporation of Cleveland, Ohio. CdS exhibits a large Hall coefficient, and the ohmic electrode contacts required for the d.c. measurements could be readily made with an indium-mercury amalgam. The sample was photoconductive and had a dark resistivity of greater than 10^{10} ohm-cm.

The photoconductivity property of the sample was employed to examine the effect of sample source impedance on the proposed experimental and analytical techniques employed in these studies. The conductivity of the sample was varied over about four orders of magnitude by changing the intensity of the optical radiation impinging on the

sample. The light source was a simple 12 volt GE #93 "high intensity" light bulb mounted in a Chemical Rubber Company reflector lamp socket and driven by a Heathkit d.c. regulated power supply. With a single 20 volt exception, the lamp was driven at a constant 15 volts to achieve the maximum conductivity desired while maintaining a constant spectral distribution of the beam. Reductions in intensity were obtained by placing a variable cross-sectional area aperture in the beam. The geometry of the sample and the entrance aperture, which replaced the vacuum system at the end of the sample chamber, was such that the sample was illuminated primarily by light reflected from the interior walls of the sample chamber assembly. No filtering of the infrared radiation was provided, but the sample and aperture assemblies were cooled by circulation of room air from a 25 cfm fan. Since the purpose of the illumination was simply to change the sample conductivity, no consideration was given to either the absolute intensity of the impinging radiation or the radiation absorbed from the beam by the sample.

A.c. and d.c. Hall measurements were alternately made on the sample at a constant illumination level. The d.c. measurements employed a battery supply for the current electrodes and a Keithley Model 601 electrometer with a 10^{14} input resistance as a detector. This high input resistance eliminates any detector loading problems and allows the

true Hall voltage V_H to be determined directly for comparison purposes. For conditions where there was no signal-to-noise problem, the a.c. signal was read on a Hewlett Packard model 302A wave analyzer. The wave analyzer scales that were used were calibrated against the calibrated display on a Tektronix model 556 oscilloscope, which has a specified accuracy of 2 percent. All impedance measurements were made with a General Radio model 1615-A capacitance bridge, which is designed to make three terminal impedance measurements conveniently and accurately.

In making three terminal a.c. measurements on resistors, considerable error can be produced by distributed capacitance from the resistor body to ground, which is represented as a lumped capacitance C_g in Fig. 10(a). In the three terminal mode only the direct impedance between the terminals is measured. Any impedance from the terminals 1 and 2 to ground is not included. However, C_g <u>does</u> affect the apparent direct impedance because it is not so simply excluded. Figure 10(b) illustrates the equivalent Π-network impedance between terminals 1 and 2, which is a capacitance C', given by

$$G' = \frac{2G_o^3}{4G_o^2 + \omega^2 C_g^2} \tag{17}$$

and

$$C' = \frac{-C_g C_o^2}{4G_o^2 + \omega^2 C_g^2} \tag{18}$$

Figure 10

Equivalent circuit of a resistor R_o showing: a) the T-representation with the distributed capacitance to ground lumped into C_g. b) the Π-representation derived by transforming the T-network in (a). C_d is the direct geometric capacitance between the resistor terminals in both cases.

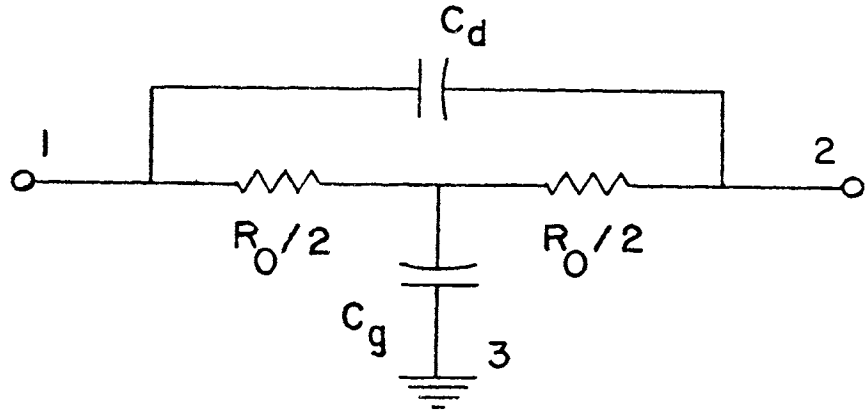

(a)

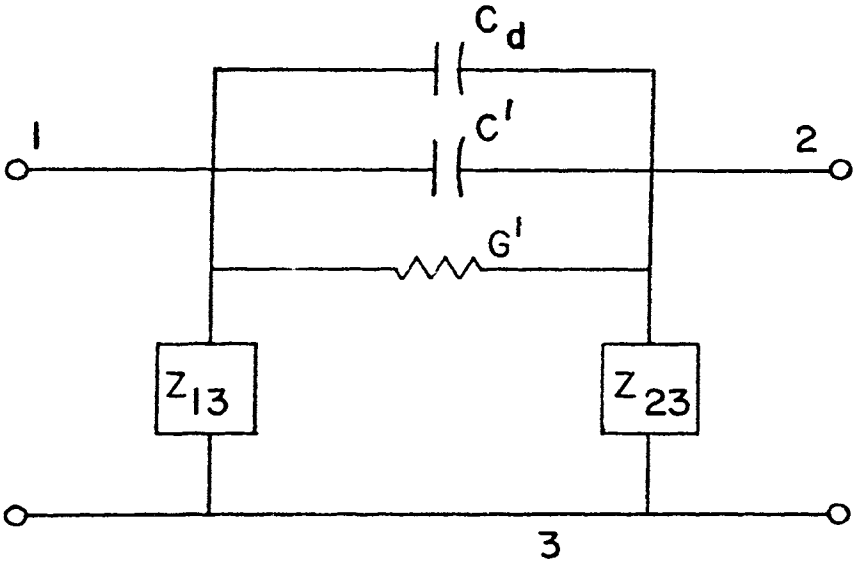

(b)

Figure 10

where $G_o = \frac{2}{R_o}$. It can be seen immediately that G' is frequency dependent and, therefore, the true value of R_o is not determined by measurement at a single frequency. However, by taking the data at different frequencies and solving the resulting equations in G', G_o and thus, R_o can be accurately determined provided the equivalent circuit used is a realistic one. In this particular work, this correction was necessary only for the lowest resistivity data and amounted to less than one percent. Data have been taken on known resistors where this effect has amounted to a 50 percent variation from 200 Hz to 1000 Hz (see Appendix A). Notice also that C' is negative, which, when placed in parallel with C_d, could give an indicated net negative capacitance. The GR1615-A bridge can indicate such a negative capacitance, and this effect has been observed both in the present data and with resistors. If, therefore, one is interested in monitoring capacitances, this feature must be kept in mind.

The resistivity is defined by the expression

$$R = \int_0^L \frac{\rho \, d\ell}{A} \tag{19}$$

here R is the measured resistance, ℓ is the sample length and A is the sample cross sectional area. For the homogeneous, rectangular parallelopiped samples used in this work the expression becomes

$$R = \frac{\rho L}{A} \tag{20}$$

Mobility is calculated from a modified form of Eq. (6), given by

$$E_H/(E_a K) = - B\mu \tag{21}$$

where K is a factor which corrects for the shunting effects of the current electrodes whenever the sample length-to-width ratio is less than four.[12]

In summary, the measurement procedure consisted of the following steps.

a) An independent measurement of the Hall voltage source resistance R_1 [Fig. 2(d)] as a function of frequency was made with the GR 1615-A impedance bridge and the data analyzed according to Eq. (17). The same technique was employed to measure the resistance of the sample between the current electrodes from which the resistivity was obtained using Eq. (20).

b) The assumed R_2, C_2 parallel equivalent input impedance was determined by measuring the ratio V_o/V_s [Fig. 2(b)] of the output voltage from the NF-1 to the input voltage from a high impedance capacitive source C_1 at frequencies displaced 25 Hz on each side of the frequency of interest and by

solving the simultaneous equations (15) and (16).

c) At each frequency of interest, the voltage was applied to the crystal, the preamp was adjusted for minimum input capacitance, and the "misalignment" voltage was removed to establish the conditions for a Hall measurement upon application of the magnetic field.

d) The magnetic field was applied in both directions and the resultant detected Hall voltage readings were averaged.

e) The d.c. Hall voltage was measured by applying a d.c. potential to the crystal and the d.c. Hall voltage was detected with the Keithley 601 electrometer.

f) The true a.c. Hall voltage V_H was calculated by substituting the experimentally determined lumped parameters, R_1, R_2 and C_2 into Eq. (9) and dividing the obtained value for F into the detected Hall voltage V_H'.

g) The mobility of the charge carriers was then calculated using Eq. (21).

IV. EXPERIMENTAL RESULTS

As described in the previous chapter, the input impedance of the detector was derived from measurements of the output voltage, V_o, obtained with a calibrated capacitive source ($C_1 = 0.00980 \pm 0.00013$pf, $R_1 >> 10^{12}$ ohms) driven by a fixed voltage source, V_s. The ratio of V_o/V_s was analyzed with a simple computer program around each center frequency to obtain the best self-consistent values of the assumed lumped R, C parallel equivalent detector input impedance over the frequency range of interest. The deduced detector input impedance is presented in Table II.

The indicated uncertainties in the tabulated values of R_2 and C_2 were based upon one's ability to reproduce the tuning characteristic of the preamplifier in order to minimize the effective shunting capacitance. It was found that at fixed V_s, V_o could be consistently reproduced with a maximum variation of $\pm 2\%$ at each frequency. This uncertainty was incorporated into any subsequently accumulated sample data since in the latter cases an independent tuning of the preamplifier was required. On the other hand, for any single set of V_o/V_s data as a function of frequency, the computer generated values of R and C were defined to better than 1%.

Upon completion of the characterization of the equivalent detector input impedance, Hall data were obtained on

Table II

R_2, C_2 parallel equivalent detector input impedance derived from the analysis of voltage ratios using a 0.00980 ± 0.00013pf capacitive source.

Frequency (Hz)	C_2, Detector Capacitance (picofarads)	X_2, Detector Reactance (10^9 ohms)	R_2, Detector Resistance (10^9 ohms)	Detector Impedance (10^9 ohms)
200	0.083 ± 0.0009	9.61 ± 0.10	11.95 ± 0.15	7.34 ± 0.14
250	0.074 ± 0.0008	8.62 ± 0.09	9.85 ± 0.13	6.48 ± 0.13
350	0.062 ± 0.0007	7.34 ± 0.08	7.65 ± 0.10	5.30 ± 0.11
400	0.058 ± 0.0007	6.87 ± 0.08	7.04 ± 0.09	4.92 ± 0.10
600	0.046 ± 0.0006	5.77 ± 0.07	5.58 ± 0.07	4.02 ± 0.08

the CdS crystal at six different resistivity levels. The data for the highest resistivity level at which complete d.c. and a.c. measurements could be made are shown in Table III. These data very clearly demonstrated the effect of detector loading. The true Hall voltage, V_H, was found to be frequency independent, which it should have been in this frequency range if the expression for $F_{X_S \to 0,\ X_l \to \infty}$ was correct. The Hall source resistance, R_l, was 1.00×10^{10} ohms for this set of data. Similar but smaller transfer function corrections were also required for the Hall voltage measured at the next two lower resistivities. No corrections were necessary for the three lowest resistivities at which measurements were made since the detector input impedance was sufficiently high that no detector loading occurred.

It is significant to note at this point that excellent apparent Hall data could be obtained from the system at resistivities higher than the 4.74×10^9 ohm-cm data (Table II). However, these data could not be corrected to give the true Hall voltage because the impedance levels at the sample were such ($>10^{11}$ ohms) that the resistance data lacked sufficient precision to allow one to compute significant values for the transfer function. Furthermore, it was not possible to make the d.c. Hall measurement because the time required to charge the electrometer input shunting capacitance from the very high resistance of the

Table III

A.c. Hall data for a CdS crystal (4.74×10^{9} ohm-cm) exhibiting a Hall source resistance of 1.00×10^{10} ohms.

Frequency (Hz)	Apparent Hall Voltage, V_H' (millivolts)	Reciprocal Transfer Function $1/\lvert F_{x_s \to 0, x_l \to \infty} \rvert$	True Hall Voltage, V_H (millivolts)
200	4.15	2.11	8.76
250	3.59	2.33	8.36
350	3.35	2.68	9.00
400	3.05	2.83	8.64
600	2.65	3.29	8.72

$\langle V_H \rangle = 8.70 \pm 0.21$ millivolts

Hall source generator was excessive. Of course, the time constant problem as such, does not affect the a.c. measurements because the detector input shunting capacitance has the effect of reducing the detected apparent Hall voltage, which was subsequently corrected by the use of the transfer function.

Table IV compares the true Hall voltages obtained independently by a.c. and d.c. measurement techniques applied to the single crystal of CdS, whose indicated resistivity was varied by photoexcitation. The data was normalized to the same applied voltage (8v) and magnetic field (5 kilogauss) for comparison purposes.

The observed apparent Hall voltage was linear with magnetic field and showed the expected phase reversal when the field was reversed. The results were quite reproducible, which is as much dependent upon one's ability to tune the neutralized capacitance amplifier consistently as any other condition.

An error analysis was performed in order to obtain information about the quality of the data. The transfer function $F_{X_s \to O,\ X_1 \to \infty}$ contains the three independent variables R_1, R_2 and C_2. The values of R_2 and C_2 were determined by the solution of the two simultaneous equations previously discussed, which could be solved to any desired accuracy consistent with the uncertainty of $\pm 2\%$ for the ratio of V_o/V_s. The actual data necessary to determine the

Table IV

Comparison of a.c. and d.c. Hall data for a single crystal sample of photoexcited CdS. B = 5 kgauss, ℓ = 9.99 mm, w = 4.34 mm, t = 1.04 mm.

V_H (d.c.) (millivolts)	V_H (a.c.) (millivolts)	Percent Difference	Resistivity (ohm - cm)	Mobility $cm^2/V \cdot sec$
8.44 $\pm$ 0.17	8.70 $\pm$ 0.23	3.1	4.74×10^9	50.5
17.1 $\pm$ 0.3	17.6 $\pm$ 0.5	2.9	5.92×10^8	102
26.6 $\pm$ 0.3	27.5 $\pm$ 0.6	3.4	8.92×10^7	158
29.8 $\pm$ 0.3	28.6 $\pm$ 0.6	4.0	3.77×10^7	173
38.2 $\pm$ 0.6	38.0 $\pm$ 0.9	0.5	1.52×10^7	225
42.6 $\pm$ 0.8	44.0 $\pm$ 1.0	3.3	6.00×10^6	248*

*Lamp driven at 20 volts for this set.

values of R_2 and C_2 involved the ratio of two voltage readings from the same meter (HP302A), and a 1% reading accuracy was typical. Therefore, the ability to reproduce these numbers to $\pm$2% was taken as their accuracy. The value of R_1 was determined from three terminal impedance measurements with the GR-1615A bridge, which had a specified accuracy of 1%.

Using the expression

$$\frac{\Delta F}{F} = \sum_{i=1}^{n} \left| \frac{\partial F}{\partial x_i} \frac{1}{F} x_i \frac{\Delta x_i}{x_i} \right| \qquad (22)$$

$\Delta F/F$ was found to be 1.2%. This value was lower than the quoted values for the individual parameters from which F was constructed because the complicated nature of the transfer function provided some compensation for the variations of the individual parameters. The measured apparent Hall voltages, V_H', were known to at least $\pm$3%. Thus, the maximum error in V_H is 4.2%. The d.c. Hall voltages have a maximum error of $\pm$2%. The calculated error in the a.c. Hall voltages plus their excellent agreement with the d.c. values shows the system accuracy can be conservatively rated at better than 5% for the determination of the Hall mobility. The resistivity is determined from an impedance measurement similar to that for R_1 and the crystal dimensions, which are known to $\pm$0.013mm corresponding to a possible 1.3% error in the smallest dimension. The

maximum error in the resistivity is less than 2.5%.

The tabulated increase in mobility as the light intensity is increased has been previously observed by R.H. Bube and H.E. MacDonald[14] in insulating materials. This was interpreted as being due to one or both of the following mechanisms: a) the occupancy of the charged scattering centers is changed as the light intensity is changed, and b) the minority carriers (in this case holes) play a continuously changing role in the conduction process as the intensity is increased. They reported that the mobility has been observed to change as much as a factor of 6 in CdS and a factor of more than 20 in CdSe under conditions of varying light intensity at room temperature.

The agreement of the a.c. and d.c. Hall voltages of Table IV indicates that the lumped parameter equivalent circuit used to represent the distributed parameters of the macroscopic sample system represents the observed behavior within the limits of inherent experimental error.

V. DISCUSSION

In view of the results presented here, the following observations and conclusions can be drawn which form the criteria that must be satisfied whenever one attempts to make a.c. Hall effect measurements on high resistivity materials which exhibit space charge polarization effects at the electrodes and where detector loading may affect the detected signal.

(a) The equivalent circuit representation of the macroscopic sample system is valid and can be used to derive the transfer function required to make corrections to the detected Hall voltage in the presence of detector loading.

(b) Regardless of the type of the detector used, the geometric capacitance associated with the sample and its electrodes adds to the detector shunting capacitance and must be taken into account. The effective input shunting capacitance contributed by the sample geometric capacitance as well as that of associated cabling may be minimized, but not eliminated, by presently available amplifiers providing capacitance compensation.

(c) Frequencies must be used such that the reactance of the space charge capacitance layer at the current electrodes is much less than the ohmic

resistance of the sample so that the applied electric field in the sample at the position of the Hall electrodes can be accurately calculated.

(d) It is desirable, though not absolutely necessary, that frequencies be used such that the reactance of the space charge capacitance layer at the Hall electrodes is much less than the ohmic resistance of the sample, which determines the equivalent Hall generator source resistance. If this condition is not satisfied at the Hall electrodes, one must characterize this capacitance layer in terms of a lumped parameter equivalent in order to include its effects in the appropriate transfer function.

(e) One must be aware that if single ended detection systems are used and the sample is driven with a voltage source, which is a characteristic consequence of high impedance sample materials, only one half of the Hall voltage is detected.

It would appear worthwhile to analyze the limited earlier literature which has been concerned with Hall effect measurements in high resistivity materials, which are susceptible to electrode space charge polarization effects and to establish the extent to which the criteria ennunciated here have received consideration. Comparisons of the

reported sensitivities for detection of the Hall signal with that of the present study would also be in order. For convenience, the discussion may be classified according to the basic experimental technique employed in the studies.

Single Frequency Technique With Guarded Input Detector

Macdonald and Robinson[4] employed the guarded input, capacitive compensated high impedance detector developed by Macdonald[3] to make a.c. Hall measurements on photo-excited electrons in radiation colored KBr. Macdonald has shown on theoretical grounds that typical apparent Hall mobilities monitored by a.c. techniques in high resistivity materials exhibiting electrode space charge polarization would be expected to exhibit a relatively constant value over an extended frequency range and to decrease from this value at both lower and higher frequencies due to the effects of electrode space charge effects and detector loading, respectively. They present frequency dependent mobility data on one sample illuminated at three different intensity levels in which the apparent Hall mobility decreases with increasing frequency, characteristic of detector loading effects. The low frequency (<200-400 Hz) limiting mobility value of 12.5 $cm^2/V \cdot sec$ was taken as the correct one since it was assumed that there were no

detector loading effects in this frequency range. The data of Onuki[5] and Kahn and Glass[13] (both of which will be discussed), and to a lesser extent, that of Redfield[6] indicate that 30 $cm^2/V \cdot sec$ is more nearly correct.

The principal assumption in choosing the plateau value of 12.5 $cm^2/V \cdot sec$ is that in this frequency range the polarization and detector loading effects are either compensating or absent. One may examine their data and obtain an explanation for the difference between the 12.5 and 30 $cm^2/V \cdot sec$ values by considering the effect of Eq. (12) which defines the transfer function associated with a measurement of this type. Their sample resistances, R_1, ranged approximately from 10^7 to 10^8 ohms, and the detector input resistance, R_2, was greater than 4×10^9 ohms. Thus, Eq. (12) can be simplified for the case $R_2 \to \infty$ and becomes

$$F_{X_1, R_2 \to \infty} = \frac{C_s}{C_2 + C_s} \left[\frac{1}{1 + j\omega \frac{R_1 C_2 C_s}{C_2 + C_s}} \right] \qquad (23)$$

This expression is in standard form for making a Bode plot[15] which describes the frequency dependence of function.

Using 30 $cm^2/V \cdot sec$ as the "correct" value and Macdonald and Robinson's low frequency limiting value of 12.5 $cm^2/V \cdot sec$, one sees that $(C_2 + C_s)/C_s = 30/12.5 = 2.4$. The quantity $(C_2 + C_s)/R_1 C_2 C_s$ is the corner frequency ,

ω_c, of the Bode plot, i.e., the frequency at which the response of $F_{X_1, R_2 \to \infty}$ is 3 db less than the low frequency limiting value. The smaller R_1, the higher will be ω_c. The highest corner frequency indicated is $\omega_c \simeq 6 \times 10^4$ Hz which corresponds to the highest light intensity and lowest $R_1 \simeq 10^7$ ohms. Using the ratio $(C_s + C_2)/C_s = 2.4$, C_2 is found to be about 4 pf which then indicates that $C_s \simeq 3$ pf. Now using the two lower corner frequencies, $\omega_c \simeq 2 \times 10^4$ Hz and 3×10^3 Hz together with the values obtained for the capacitances C_s and C_2, one finds values for R_1 of about 3×10^7 and 2×10^8 ohms, respectively, which are consistent with their reported values. Whenever one realizes that with a guarded input detector C_2 contains the detector shunting capacitance (0.3 pf) and C_{13} plus C_{15} (Fig. 3), each typically being 1-2 pf, the value of 4 pf is reasonable. Furthermore, Onuki[5] reports the space charge capacitance in KBr is approximately 150 pf/cm^2 for silver paint electrodes. The value $C_s \simeq 3$ pf implies a reasonable 0.02 cm width line of contact for the knife edge electrode employed by Macdonald and Robinson across the 1 cm thick sample. Thus, the data of Macdonald and Robinson is consistent with and can be interpreted readily on the basis of a space charge capacitance at the Hall electrodes and detector loading effects, neither of which was considered in their work.

They also present one set of data for an additively colored KBr sample in which the apparent mobility decreases at both low (<150 Hz) and high (>1 KHz) frequencies with a plateau between corresponding to 7.5 $cm^2/V.sec$. Though insufficient data is available to arrive at component values, this characteristic shape and reduced plateau is predicted by Eq. (12), when R_1 is of the same order of magnitude as R_2.

Thus, one concludes that the plateau in apparent mobility measurements may or may not correspond to true mobility, depending upon the magnitude of detector loading corrections and space charge effects.

Macdonald and Robinson were able to null the "misalignment" voltage to approximately 1 mv which corresponds to a detection sensitivity of $V_H(min)/V_a \simeq 10^{-5}$, assuming they were using their maximum value of $V_a = 100$ volts. This may be compared to the values 1.8×10^{-7} and 8.7×10^{-7} (Table I) at 10^7 and 10^8 ohms sample impedances, respectively, which were obtained in the present work.

Onuki[5] later employed the experimental technique of Macdonald and Robinson to measure the temperature dependence of the Hall mobility of photoexcited electrons in KBr over the range 80 K< T< 280 K at a single frequency (330 Hz) which was considered to be sufficiently high to minimize space charge polarization effects at the electrodes.

He was aware of the problem of detector loading and applied a correction to his measured Hall signal, V_H', of the form $V_H = [(Z_D + Z_H)/Z_D]\, V_H'$, where Z_D was the measured detector input impedance ($\sim 8 \times 10^7$ ohms) and Z_H was the measured impedance between the two Hall electrodes (~ 1 to 3×10^9 ohms at room temperature).

Onuki used single ended detection and therefore actually measured only one-half of the generated Hall signal in view of the condition of a voltage driving source associated with the high sample impedance. This condition also requires that Z_H be measured between one Hall electrode and the current electrodes which are tied together as indicated by Fig. 4, rather than across the two Hall electrodes which corresponded to Onuki's measurement. Even Onuki's approximate correction should have read $V_H = 2(Z_D + Z_H')/Z_D\, V_H'$, where Z_H' is the impedance between <u>one</u> Hall electrode and the <u>two</u> current electrodes. From Onuki's typical sample geometry, one may show $Z_H' = Z_H/(0.6 + 0.045\ \text{cm}/d)$ where d is the width of the Hall electrode. For d of the order of 1/10 of the sample length of 0.40 cm, one observes that $Z_H' \sim (1/2) Z_H$ and the two errors introduced by Onuki tend to compensate one another. The net result is the generation of Hall mobility data that compares favorably with that of Kahn and Glass [13] (room temperature) who employed a more indirect method of

measurement, and the low temperature data of Redfield[6], obtained with the transient pulse Hall technique.

Two additional inconsistencies appear in Onuki's data. The temperature dependent correction factors deduced from his data differ by a factor of twenty for two different samples of similar geometries. Such a variation cannot be resolved from an analysis of potential errors in the described experimental technique. Also, the temperature dependence of his reported "conductivity" data ($\sigma = 1/Z_H$) does not conform with that predicted by theory for the specific conductivity of any known class of solids, photoexcited or otherwise. If σ is considered to be the real part of the admittance, then its temperature dependence, which contains both a resistive and reactive contribution is sufficiently complicated to provide the possibility of generating the inflexion observed in the data. The same statement holds if the data presented actually correspond to $\sigma = 1/|Z_H|$. However, information on the activation energies for carrier diffusion and the bimolecular recombination coefficient of electrons and F-centers is not available, and no detailed analysis of his experimental results is feasible.

Onuki reports the maximum sensitivity of "the device" was 3×10^{-3} volts/ma. Using the reported impedance between the current electrodes of about 10^{10} ohms and

his maximum applied voltage, V_a, of 200 volts, one finds that $V_H(min)/V_a \simeq 3 \times 10^{-10}$. This value is very low and is apparently not representative of the entire system because Onuki reports mobility values of 27 $\pm$ 5 and 31 $\pm$ 6 $cm^2/V \cdot sec$ for two individual samples at room temperature. Using $\Delta\mu = 5$ $cm^2/V \cdot sec$ as the system capability, B = 4500 gauss, and $\ell/Kw = 3.3$, for Onuki's system, one finds $V_H(min)/V_a = 6.8 \times 10^{-5}$ which is of the same order of magnitude as that obtained in this work at 10^9 ohms (Table I). This value for $V_H(min)/V_a$ is the one which should be used since it is certainly more indicative of the quality of the final results which could be obtained with his Hall effect measurement system. In Onuki's work, the capacitances C_{15} and C_{13} also add to the detector input shunting capacitance as shown in the discussion of Macdonald and Robinson's work. However, in view of the already low detector input impedance of Onuki's detector, the capacitances C_{13} and C_{15} were relatively unimportant.

Double Frequency Technique

Russell and Wahlig[9] first proposed a double frequency a.c. technique for making Hall coefficient measurements. By driving the magnetic field at 60 Hz and the current electrode voltage at 70 Hz, they were able to analyze the Hall signal generated at the difference frequency after

introducing adequate bucking sections to minimize the undesired mixing occurring throughout the circuit. The technique was applied to semiconducting materials having resistances of less than a few thousand ohms. For their 2×10^3 gauss magnetic field, they quote an anticipated mobility sensitivity of 1 $cm^2/V \cdot sec$ corresponding to a $[V_H/V_a] \times [\ell/(Kw)] = 2 \times 10^{-5}$ for their low ($\leq 3 \times 10^3$ ohm) resistance materials. The present results demonstrate a capability of obtaining a $V_H(min)/V_a = 2 \times 10^{-9}$ at a sample resistance level at least one hundred times higher. The geometric factor $[\ell/(Kw)]$, which involves the sample length (ℓ), width (w) and the Isenberg, Russell and Greene [12] Hall correction K, ranges from 1 to 10 for typical sample systems. The presently reported technique represents an approximately three order of magnitude improvement over the method employed by Russell and Wahlig.

Read and Katz [8] have briefly outlined a modification of the Russell and Wahlig [9] technique which they applied to measurements of the apparent Hall mobility of NaCl over the temperature range from 610 to 780 C. A referenced elaboration scheduled for subsequent publication has never appeared in print. They incorporated an ultralinear cathode follower circuit designed by Read[16] to minimize mixing of the 85 Hz current electrode voltage and the 60 Hz magnetic field drive which was used to generate the monitored 25 Hz Hall signal. Hall mobility was calculated

from the voltage (V_a) applied to the current electrodes and the geometrically corrected (after Isenberg, Russell and Greene[12]) measured Hall voltage (V_H') together with the applied magnetic field (B);

$$\mu = \left(\frac{\ell}{Kw}\right)\left(\frac{V_H'}{B\ V_a}\right) = 2.10\left(\frac{V_H'}{B\ V_a}\right) \qquad (24)$$

Their data falls in the range of that obtained with ion drift mobility measurements. Although NaCl characteristically exhibits electrode space charge polarization effects, no mention is made of any attempts to eliminate or minimize the errors associated with this effect in their study. Furthermore, there is no indication that any attempts were made to minimize the shunting input capacitance of their assumed high input resistance Hall signal detector which could result in detector loading. In view of the previously described results of the present paper, it would appear worthwhile to examine the possibility of error introduced by these effects in the Read and Katz study.

An estimate of the error, introduced by assuming that the electric field is uniform between the current electrodes and can be represented by the ratio of the applied voltage (V_a) to the geometric length (ℓ) of the sample, can be obtained from literature data on the properties of NaCl. One may extrapolate a zero frequency space charge

capacitance, C_o, of 240 pf cm^{-2} at 331 C from the data of Wimmer and Tallan[17] and employ this without frequency modification at the low frequencies quoted in the Read and Katz study. It can be shown (see Appendix B) from the theory of Macdonald[10] and the data of Rothman, et. al.[18], that the corresponding capacitances at the limits of the temperature range are C_o(610 C) = 7.3×10^3 pf cm^{-2} and C_o(780 C) = 2.4×10^4 pf cm^{-2}. Biermann's data[19] for the resistivity of "pure" NaCl give approximately ρ(610 C) $\simeq 7 \times 10^4$ ohm•cm and ρ(780 C) $\simeq 2 \times 10^3$ ohm•cm. No data on specific sample geometry are given by Read and Katz other than the statement that samples were "square"; however, the value of $[\ell/(Kw)] = 2.10$ used in their calculations corresponds to an $\ell/w \simeq 2$, so we may assume sample dimensions of ℓ= 1.0 cm, w = 0.5 cm and t = 0.5 cm. The sample equivalent series R_l, C_s impedance component values [Fig. 2(a)] across the current electrodes at 85 Hz are R_l(610 C) $\simeq 3 \times 10^5$ ohms, X_s(610 C) $\simeq 2 \times 10^6$ ohms and R_l(780 C) $\simeq 8 \times 10^3$ ohms, X_s(780 C) $\simeq 6 \times 10^5$ ohms. Thus, $7 < X_s/R_l < 75$ and most of the voltage drop occurs at the current electrodes. Therefore, the assumed V_A/ℓ used to compute the mobility does not represent the voltage gradient at the Hall electrode position near the center of the sample ($\sim \ell/2$).

To examine possible errors in measurements at the Hall electrodes, it is useful to consider $V_H = 2V_H'/F$, where

V_H and V_H' are the true and measured Hall voltages, respectively, F is the appropriate transfer function which depends upon the degree of detector loading, and the factor of 2 is contributed by the fact that the high sample impedance ($>10^5$ ohms) results in a voltage driving source, and with single ended detection only one half of the Hall signal is detected. Assuming that the sample resistance between the Hall electrodes is of the same order as that between the current electrodes ($\leq 10^5$ ohms) and small compared with the electrode space charge reactance and detector input impedance, the transfer function given in Eq. (11) becomes

$$\frac{1}{F_{X_1 \to \infty}} = 1 + \frac{X_s}{X_2} + j \frac{X_s}{R_2} \qquad (25)$$

Assuming a typical Hall electrode width of about 0.1 mm , one obtains for the space charge capacitance the values $X_s(610\ C) \simeq 3 \times 10^8$ ohms and $X_s(780\ C) \simeq 1 \times 10^8$ ohms at the 25 Hz Hall signal frequency. Read and Katz do not describe the input characteristic impedance of their detector but it is known from Read's work[16] that although it could be made to have a high input resistance, it did not incorporate capacitance compensation. For a typical cable capacitance of 64 pf, X_2 at 25 Hz is 1×10^8 ohms. Assuming $R_2 >> 10^8$ ohms, one finds $1/F_{X_1 \to \infty}$ (610 C) $\simeq 4$, $1/F_{X_1 \to \infty}$ (780 C) $\simeq 2$. The expression for calculating μ which incorporates these

corrections is given by :

$$\mu(T) = \left[\frac{\ell}{KwB}\right]\left[\frac{2}{F(T)}\right]\left[\frac{(R_1^2(T)+X_s^2(T))^{\frac{1}{2}}}{R_1(T)}\right]\frac{V_H'(T)}{V_a'} \qquad (26)$$

where $V_H'(T)$ and V_a' are the measured Hall voltage and the measured voltage applied to the current electrodes. Substituting for $F(T)$, $R_1(T)$ and $X_s(T)$, one obtains

$$\mu(610\ C) \simeq 56\left[\frac{\ell}{Kw\ B}\right]\frac{V_H'(610\ C)}{V_a'} = 56\ \mu_{RK}(610\ C) \qquad (27)$$

$$\mu(780\ C) \simeq 300\left[\frac{\ell}{Kw\ B}\right]\frac{V_H'(780\ C)}{V_a'} = 300\ \mu_{RK}(780\ C) \qquad (28)$$

where μ_{RK} are the values reported by Read and Katz.

The conservative correction factors that this analysis predicts for the data of Read and Katz are not only large but would effectively increase their reported activation energy for the Hall mobility by a factor of about five. The variation ($\simeq$10) of applied electric field, V_a'/ℓ, with temperature in the region of the Hall electrodes should have been sufficient to make the observed Hall signal decrease with increasing temperature for the factor of four increase in μ_{RK} which would be consistent with typical mobility activation energies ($\sim$0.8 ev) in this temperature range. It does not appear possible to resolve the absence of this

effect in view of the space charge polarization that must have existed at the electrodes. The partial compensation afforded by the temperature dependence of the transfer function is insufficient to cancel the effects at the current electrodes. The failure of Read and Katz to submit the scheduled subsequent elaboration of their work for publication may be related to problems arising from considerations similar to those mentioned here.

Read and Katz report a detectable Hall voltage sensitivity of 5×10^{-8}v, and an analysis of their mobility uncertainties suggests that the driving voltage was between 5 and 50v. Thus, $10^{-9} < V_H(\text{min})/V_a < 10^{-8}$ at effective sample impedances of 10^6 ohms (assuming the capacitance reactance is present and dominates) compared to the present results of $2 \times 10^{-9} < V_H(\text{min})/V_a < 9 \times 10^{-9}$ at sample resistances of 10^5 and 10^6 ohms, respectively.

Transient Pulse, Null Detection Technique

Redfield[6] developed a transient pulse null technique for measuring the mobility of photoexcited charge carriers in diamond and the alkali halides. Ahrenkiel and Brown[7] also employed this same basic technique with some experimental modifications to measure the mobility of photoexcited electrons in the alkali halides.

Redfield provides a very complete discussion of the

technique. The basic features are illustrated in a schematic fashion in Fig. 11 and consist of the following:

(a) A light pulse is used to excite the charge carriers into the conduction band.

(b) The applied field is produced in the crystal by the voltage, V_a, applied across (not between) the semiconducting electrodes on either side of the sample, which is in a magnetic field.

(c) A charge flow between the electrodes produced by the Hall effect is detected by the charge detector (A).

(d) The value of the Hall voltage is then the value of the series voltage (B) required such that no charge flow is indicated (A) whenever the light is pulsed on.

The technique is relatively inaccurate at low mobility values. Redfield [6] reports a minimum mobility value of 25 $cm^2/V \cdot sec$ with $\pm$ 100% uncertainty. Ahrenkiel and Brown [7] report a minimum resolvable mobility of 50 $cm^2/V \cdot sec$ with an uncertainty of $\pm$ 50%. This relatively high minimum resolvable mobility can be explained on the basis of detector loading using the equivalent circuit of Fig. 2(d). The Hall voltage source, V_H, is now a pulse generator; R_1 is the output resistance of the Hall source; and R_2 and C_2 still represent the input impedance of the

Figure 11

Schematic representation showing the basic features of the Redfield transient pulse, null technique. The vector diagram indicates the relative directions of the fields involved. A is the charge detector, B is the variable series voltage, C is the sample with semiconducting transparent electrodes on each side.

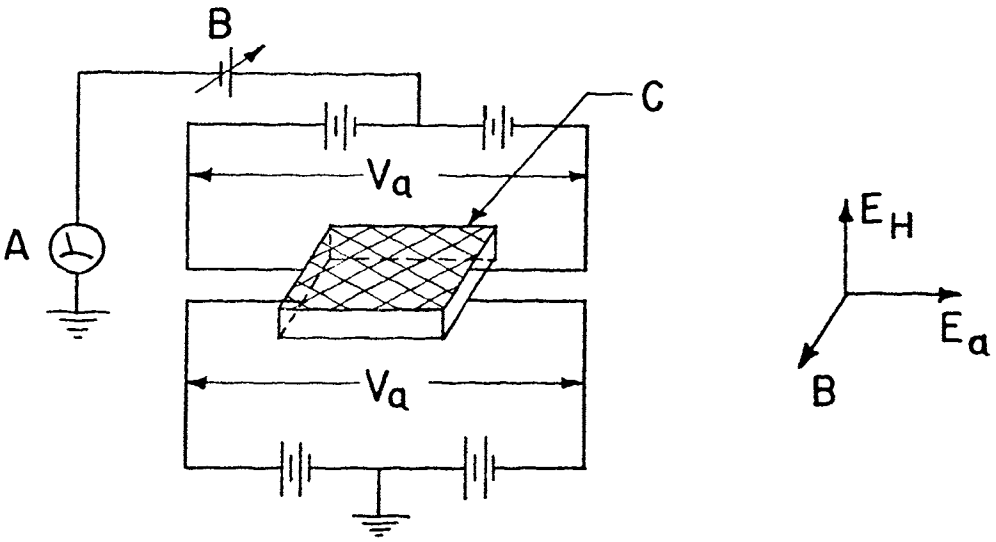

Figure 11

charge detector. Since this is a null technique, the relative values of R_1 and the input impedance of the charge detector are not a primary consideration.

The minimum resolvable mobility for any given set of conditions is determined by the minimum charge sensitivity of the detector, which determines the resolution at the null point. If C_2 is large, the minimum charge sensitivity is raised because more charge is required to raise the voltage to a measurable level at the detector input. Since the quantity of charge flow per pulse of light is fixed, it is apparent that the minimum resolvable mobility would be lowered in direct proportion to the extent to which C_2 could be reduced. Incorporation of a neutralized input capacitance preamplifier would be an effective means of reducing C_2 as has been shown in the present work.

Redfield and Ahrenkiel and Brown worked with sample impedances of approximately 10^7 ohms. The results of the present study (Table I) indicate a $V_H(\text{min}) \simeq 1.3 \times 10^{-6}$ volts at 10^7 ohms for unity signal-to-noise which corresponds to a mobility of about 5×10^{-3} $cm^2/V \cdot sec$ for a length-to-width ratio of 2.5. This is in marked contrast to the value (30 $cm^2/V \cdot sec$) available with the pulse technique. One should also note that the pulse technique is limited to photoconductivity studies and that thin samples are required to avoid errors due to fringing effects at the sample edges.

Mobility Deduction From A.C. Impedance Measurements

Kahn and Glass[13] have used the equivalent circuit of Fig. 2(a), which is derivable from Macdonald's theory[10] for space charge conduction, to deduce the mobility and concentration of photoexcited electrons in additively colored KBr. This is accomplished by making impedance measurements as a function of frequency on the sample and fitting the real part of the data to the first term in Eq. (10) and the imaginary part to the remaining terms of Eq. (10) to find G_1 and C_s (C_∞ and C_o in the notation of Kahn and Glass, and Macdonald). The ohmic conductance G_1 yields the conductivity directly and C_s yields the charge carrier concentration which allows one to obtain the mobility.

The material in question must satisfy certain conditions, however, before the above technique can be used. These conditions are:

(a) No charge may flow through the electrode sample interface; i.e., totally blocking electrodes.

(b) The usual equations for diffusion conductivity must apply.

(c) The ionization rate constant is much smaller than the recombination rate constant, i.e., low dissociation.

(d) Bimolecular recombination is assumed.

The data presented by Kahn and Glass seem to indicate the above conditions were reasonably met in KBr, and they report a mobility of 32.2 $cm^2/V \cdot sec$. It should be noted that there is no direct method of checking the results obtained in this manner other than by Hall effect measurements, and many materials of interest do not satisfy the necessary conditions for use of this technique, especially the requirement for totally blocking electrodes.

VI. CONCLUSIONS

On the basis of the present experimental results and an analysis of the existing literature concerning Hall effect measurements in high resistivity materials exhibiting electrode space charge polarization effects, the following conclusions appear to be in order.

It is possible to design an a.c. detection system employing a capacitive compensation feature which reduces the detector shunting capacitance, referenced to the sample electrodes, to a small (<0.1 pf) and accurately definable value compatible with a.c. measurements over a frequency range extending up to a few KHz. Effective detector input impedances of 4×10^9 to 7×10^9 ohms have been demonstrated at frequencies of 600 and 200 Hz, respectively.

Lumped parameter equivalent circuit elements have been developed to approximate the true, but unmeasurable, distributed parameters associated with a typical macroscopic sample system. Independent measurements of the lumped equivalent parameters allow one to select the lowest signal frequencies required to sufficiently minimize space charge polarization effects at the sample electrodes and to accurately analyze the corrections required to obtain the true Hall signal from the measured value, which may be biased by the effects of detector loading and the Hall source configuration in the sample.

The utility of the proposed equivalent circuits has been demonstrated by studies of the Hall mobility of carriers in photoexcited CdS. Ohmic contacts can be made to CdS, and a.c. and d.c. measurements agreed within a maximum difference of 4% after applying experimentally determined. Hall signal transfer function correction factors of up to 3.29 in the a.c. data.

It has been demonstrated that when space charge polarization effects are sufficiently minimized at the electrodes, the Hall source generator impedance can be treated as a pure resistance. This result provides a considerable simplification of the transfer function required to obtain the true Hall signal from the measured data. This result also appears to be justified by the observation that there is no apparent physical reason why the transport properties of the charge carriers should depend upon the dielectric constant in such a way as to cause the output impedance of the equivalent Hall source generator to exhibit a reactive component.

It has been noted that for high impedance sample materials , the signal generator driving the sample appears as a voltage source because of its relatively low output impedance. If single-ended detection of the Hall signal is employed in this case, only one half of the Hall signal will be detected. Furthermore, the Hall source resistance required in the transfer function to correct the measured

Hall signal corresponds to a measurement between the detector Hall electrode and both of the current electrodes, these being coupled together. Analysis of existing literature has shown that this feature of the measurement has not been appreciated, and unrecognized errors of a factor of two have been incorporated into the Hall measurements. Furthermore, whenever the driving source appears as a voltage source to the sample, the interelectrode capacitances between the Hall and current electrodes add directly to the detector shunting capacitance, which increases the detector loading of the Hall signal. Capacitive compensated preamplification of the type described in the present work provides maximum capacitive neutralization down to and including these interelectrode capacitances, and this technique is much to be preferred over previous guarded input, cathode follower types whose neutralization capability only extends through the detector cabling. Also, it should be noted that in high impedance samples, Hall data discussions should be restricted to consideration of the Hall <u>angle</u> only, rather than the Hall coefficient, since the latter implicitly assumes a current rather than a voltage source as viewed by the sample.

The existing literature has been critically reviewed on the basis of the results of the present study. Analysis of the data of Macdonald and Robinson has shown that their

apparently low values for the Hall mobility of photoexcited electrons in KBr can be explained by the presence of neglected detector loading. The work of Onuki on KBr has been shown to contain two large and approximately compensating errors associated with incorrect analysis of the effects of detector loading and failure to recognize that the single-ended detection techniques employed actually measured only one half of the Hall signal in this material. Both of these studies employed the guarded input, cathode follower detector and each failed to recognize the inherent detector shunting introduced by the sample interelectrode capacitances. The relatively poor Hall signal resolution reported by Redfield, and Ahrenkiel and Brown using transient pulse, null detection techniques to study the mobilities of photoexciited carriers in diamond and the alkali halides can be explained by the present work in terms of detector loading. Suggestions for improving the resolution of this otherwise fine technique by minimizing the input capacitance of the null detector have been provided.

The sensitivity of the present technique for the detection of an a.c. Hall signal in high resistivity materials has been shown to be equal to or better than that reported in the existing literature. Of even greater significance, however, is the ability of the present technique to correct these measured data to obtain the

information necessary to predict the true physical properties of materials under investigation.

Finally, this study suggests that further improvements in a.c. Hall measurements will be provided by improvements in the dynamic range of available impedance bridges and improvements in the drift properties of available a.c. signal generators. The present detection technique and the apparent validity of the lumped parameter, equivalent circuits developed in this study are capable of generating corrected Hall signal data for materials exhibiting impedances a couple of orders of magnitude larger than those studied to date if more sensitive a.c. bridges become available to specify the value of the circuit parameters required in the transfer function employed to correct the measured Hall signal data.

APPENDIX A

THREE TERMINAL IMPEDANCE MEASUREMENTS

In making three terminal impedance measurements on resistors, considerable error can be produced by the distributed capacitance between the resistor body and ground. Through the use of equivalent circuits, such as given in Fig. 10, it is possible to analyze the frequency dependence of the real and/or imaginary part of the impedance seen at the terminals and obtain the quantities of interest. However, the equivalent circuit of Fig. 10 is not universal and does not always apply beyond even a very limited frequency range.

Table A-I tabulates the data obtained from an impedance measurement on a 10^9 ohm resistor in the three terminal mode. A computer program was written to select the best value of G_o and C_g in Eq. (17) to fit the measured conductance G'. Any combination of points up to 1 KHz gave very good results as can be seen by examining Table A-II. However, any set containing the 5 KHz point gave very poor results showing that the assumed equivalent circuit is not valid up to 5 KHz. No additional points were tried and the additional data are presented to illustrate that G' displays a nearly constant value from 5 to 20 KHz which Eq. (17) does not predict.

To further illustrate the difficulties which can be experienced, data are presented in Table A-III for a 10^8 ohm

Table A-I

The data taken on a $1.00 \times 10^{9}\ ^{-0}_{+2}\%$ ohm resistor in the three terminal mode. $C = C_d + C'$.

Frequency (Hz)	C (pf)	G' (μ mho)
200	-0.1349	.000964
500	-0.1146	.000822
10^3	-0.0729	.000541
5×10^3	-0.00403	.000140
10×10^3	-0.00043	.000133
13×10^3	0.0002	.000133
15×10^3	0.00018	.000134
20×10^3	0.00038	.000136

Table A-II

Results of a computer fit of the data of Table A-I to Eq. (17) to determine R_0.

Combination of Points Used (Hz)	R_0 (10^9 ohms)
200, 500	1.003
500, 1000	1.006
1000, 5000	1.63
200, 500, 1000	1.004
200, 500, 1000, 5000	1.258

Table A-III

Data taken on a $1.00 \times 10^8 \pm 1\%$ ohm resistor in the three terminal mode. $C = C_d + C'$.

Frequency	G' (μmho)	C (pf)
200	.00873	-3.250
400	.00568	-2.558
600	.00265	-1.844
800	.00025	-1.236
900	-.00056	-1.007
1000	-.00125	-0.804

resistor with a much longer body than the 10^9 ohm resistor. Notice that G' goes negative between 800 and 900 Hz.

E.W. Rusche[20] has found that an equivalent circuit for a resistor with two capacitances to ground similar to that of Fig. 10(a) predicts a negative conductance upon making the two required transformations to arrive at a Π-network equivalent circuit analogous to that in Fig. 10(b).

Thus, when making three terminal impedance measurements, care must be taken to insure that errors are not introduced by the experimental configuration itself.

APPENDIX B

SPACE CHARGE CAPACITANCE TEMPERATURE DEPENDENCE

In the theory of space charge polarization of Macdonald[10], the zero frequency space charge capacitance per unit area is given by

$$C_0 = \frac{\varepsilon}{4\pi L_D} \tag{B-1}$$

where L_D is the Debye length given by

$$L_D = [\varepsilon kT/(4\Pi e^2 c_o)]^{1/2} \tag{B-2}$$

where ε is the dielectric constant, k is Boltzmann's constant, T is the temperature (K), e is the electronic charge, and c_o is the charge concentration. The temperature range of 600-800 C for NaCl is in the region of intrinsic conduction ($n_o \simeq p_o \equiv c_o$) and c_o is of the form

$$c_o = A \exp(-E_f/2kT) \tag{B-3}$$

where E_f is the energy of formation of a Schottky defect pair. Substituting Eq. (B-3) into Eq. (B-2) and this result into Eq. (B-1), one obtains the expression for C_0.

$$C_0 = 1/2 \left[\frac{\varepsilon e^2 A}{\Pi k}\right]^{1/2} \left[\frac{e^{-E_f/kT}}{T^{1/2}}\right] \tag{B-4}$$

Using the data of Wimmer and Tallan[17] on NaCl, $C_0(331\ C)$ = 240 pf/cm^2, the temperature dependence of C_0 is given by

$$\frac{C_0(T)}{C_0'(331\ C)} = \left[\frac{(T')^{1/2}}{e^{-E_f/T'}}\right]\left[\frac{e^{-E_f/kT}}{T^{1/2}}\right]$$

Using Rothman, et. al.[18] data, E_f = 2.38 ev/atom and $k = 8.64 \times 10^{-5}$ ev/(K · atom) the required values of $C_0(610\ C) = 7.3 \times 10^3$ pf/cm^2 and $C_0(780\ C) = 2.4 \times 10^4$ pf/cm^2 used in the analysis of Read and Katz's work[8] can be found.

REFERENCES

1. P. Suptitz and J. Teltow, Phys. Stat. Sol. 23, 9 (1967).
2. Solid State Electrochemistry by D.O. Raleigh in "Progress in Solid State Chemistry" edited by H. Reiss, Pergamon Press (1967).
3. J. R. Macdonald, Rev. Sci. Instrs. 25, 144 (1954).
4. J. Ross Macdonald and J.E. Robinson, Phys. Rev. 95, 44 (1954).
5. M. Onuki, J. Phys. Soc. Japan 16, 981 (1961).
6. A.G. Redfield, Phys. Rev. 94, 526, 537 (1954).
7. R.K. Ahrenkiel and F.C. Brown, Phys. Rev. 136, A223 (1964).
8. P.L. Read and E. Katz, Phys. Rev. Letters 5, 466 (1960).
9. B.R. Russell and C. Wahlig, Rev. Sci. Instr. 21, 1028 (1950).
10. J.R. Macdonald, Phys. Rev. 92, 4 (1953).
11. D.E. Harnett and N.P. Case, Proc. IRE 23, 578 (1935).
12. I. Isenberg, B.R. Russell and R.F. Greene, Rev. Sci. Instrs. 19, 685 (1948).
13. D. Kahn and A.J. Glass, J. Phys. Chem. Solids 17, 210 (1961).
14. R.H. Bube and H.E. MacDonald, Phys. Rev. 121, 473 (1961).

15. B.C. Kuo, *Automatic Control Systems*, (Prentice-Hall, Inc., Englewood Cliffs, N.J., 1962) Chapter 6.

16. P.L. Read, Rev. Sci. Instr. 31, 979 (1960).

17. J.M. Wimmer and N.M. Tallan, J. Appl. Phys. 37, 3728 (1966).

18. S.J. Rothman, L.W. Barr, A.H. Rowe and P.G. Selwood, Phil. Mag. 14, 501 (1966).

19. W. Biermann, Z. Phys. Chem. N.F. 25, 90 (1960).

20. Private communication. E.W. Rusche, P.O. Box 698, San Diego, California, 92116.

VITA

James Dale Boyd was born in Decatur, Illinois, on October 4, 1940. He grew up on a farm and received his primary and secondary education in the Argenta-Oreana Community Unit School System. Upon completion of his secondary education, he received an Illinois State scholarship and attended Millikin University in Decatur for two years. He then transferred to the University of Illinois and received a B.S. in Engineering Physics in 1962, and an M.S. in Electrical Engineering in 1963. After a short period of employment with Caterpillar Tractor Co., he came to the University of Missouri at Rolla in 1964, where he received a research fellowship with the Graduate Center for Materials Research, which he has held continuously. He has been elected to Sigma Tau and Sigma Xi.

He is married to the former Verla Glover of Alton, Illinois, and they have two children, J. Dale, Jr., and Marcena Lea.